National Library of Canada
Canadian Theses Service
Ottawa, Canada
K1A 0N4

Bibliothèque nationale du Canada
Services des thèses canadiennes

CANADIAN THESES

THÈSES CANADIENNES

NOTICE

The quality of this microfiche is heavily dependent upon the quality of the original thesis submitted for microfilming. Every effort has been made to ensure the highest quality of reproduction possible.

If pages are missing, contact the university which granted the degree.

Some pages may have indistinct print especially if the original pages were typed with a poor typewriter ribbon or if the university sent us an inferior photocopy.

Previously copyrighted materials (journal articles, published tests, etc.) are not filmed.

Reproduction in full or in part of this film is governed by the Canadian Copyright Act, R.S.C. 1970, c. C-30.

AVIS

La qualité de cette microfiche dépend grandement de la qualité de la thèse soumise au microfilmage. Nous avons tout fait pour assurer une qualité supérieure de reproduction.

S'il manque des pages, veuillez communiquer avec l'université qui a conféré le grade.

La qualité d'impression de certaines pages peut laisser à désirer, surtout si les pages originales ont été dactylographiées à l'aide d'un ruban usé ou si l'université nous a fait parvenir une photocopie de qualité inférieure.

Les documents qui font déjà l'objet d'un droit d'auteur (articles de revue, examens publiés, etc.) ne sont pas microfilmés.

La reproduction, même partielle, de ce microfilm est soumise à la Loi canadienne sur le droit d'auteur, SRC 1970, c. C-30.

THIS DISSERTATION HAS BEEN MICROFILMED EXACTLY AS RECEIVED

LA THÈSE A ÉTÉ MICROFILMÉE TELLE QUE NOUS L'AVONS REÇUE

Canada

NL-339 (r. 86/06)

THE UNIVERSITY OF ALBERTA

SENSITIZER ADDUCTS TO MOUSE TISSUES AS A PROBE FOR CELLULAR pO_2

by

DEBORA JOAN VAN OS - CORBY

A THESIS

SUBMITTED TO THE FACULTY OF GRADUATE STUDIES AND RESEARCH

IN PARTIAL FULFILLMENT OF THE REQUIREMENTS FOR THE DEGREE

OF MASTER OF SCIENCE

IN

EXPERIMENTAL RADIOLOGY

DEPARTMENT OF RADIOLOGY AND DIAGNOSTIC IMAGING

EDMONTON, ALBERTA

SPRING, 1986

Permission has been granted to the National Library of Canada to microfilm this thesis and to lend or sell copies of the film.

The author (copyright owner) has reserved other publication rights, and neither the thesis nor extensive extracts from it may be printed or otherwise reproduced without his/her written permission.

L'autorisation a été accordée à la Bibliothèque nationale du Canada de microfilmer cette thèse et de prêter ou de vendre des exemplaires du film.

L'auteur (titulaire du droit d'auteur) se réserve les autres droits de publication; ni la thèse ni de longs extraits de celle-ci ne doivent être imprimés ou autrement reproduits sans son autorisation écrite.

ISBN 0-315-30243-7

THE UNIVERSITY OF ALBERTA

RELEASE FORM

NAME OF AUTHOR: DEBORA JOAN VAN OS - CORBY

TITLE OF THESIS: Sensitizer Adducts to Mouse Tissues as a Probe for Cellular pO_2

DEGREE FOR WHICH THESIS WAS PRESENTED: MASTER OF SCIENCE

YEAR THIS DEGREE GRANTED: 1986

Permission is hereby granted to THE UNIVERSITY OF ALBERTA LIBRARY to reproduce single copies of this thesis and to lend or sell such copies for private, scholarly or scientific research purposes only.

The author reserves other publication rights, and neither the thesis nor extensive extracts from it may be printed or otherwise reproduced without the author's written permission.

Debora Joan Van Os - Corby

PERMANENT ADDRESS: 402, 2211 - 118 Street

Edmonton, Alberta

DATED: December 1, 1985

THE UNIVERSITY OF ALBERTA

FACULTY OF GRADUATE STUDIES AND RESEARCH

The undersigned certify that they have read, and recommend to the Faculty of Graduate Studies and Research for acceptance, a thesis entitled "Sensitizer adducts to mouse tissues as a probe for cellular pO_2" submitted by Debora Joan Van Os - Corby in partial fulfillment of the requirements for the degree of Master of Science in the Department of Radiology and Diagnostic Imaging.

Supervisor: J.D. Chapman, Ph.D.

Internal Examiner: C.J. Koch, Ph.D.

Internal Examiner: V. Paetkau, Ph.D.

Internal Examiner: G.O. Bain, M.D.

DATE: December 16, 1985

Internal Examiner: R.L. Jones, Ph.D.

DEDICATION

To my husband Cliff, for his constant encouragement and support.

ABSTRACT

A recent study by Garrecht and Chapman (21), described the distribution of the radiosensitizer ^{14}C-Misonidazole in Balb/C mice. After multiple injections of drug it was determined using both autoradiographic and scintillation procedures that the level of ^{14}C retained in the tumor was 2 - 15 times higher than that retained in all other normal tissues except liver. The level of ^{14}C retained in liver was similar to that found in tumor. This thesis presents studies designed to determine if the increased binding observed to liver *in vivo* was due to decreased liver oxygenation or to a distinctive enzyme complement associated with drug detoxification. In addition, the feasibility of using the sensitizer adduct technique as a means to determine the pO_2 of tissues at the cellular level was examined.

An *in vitro* comparison of the binding rates of ^{14}C-Misonidazole to EMT-6 tumor cells, hepatoma cells, V79 cells and mouse hepatocytes showed that, at all drug concentrations studied, mouse hepatocytes exhibited the lowest rate of binding. These studies suggest that mouse hepatocytes do not contain a unique complement of nitroreductase enzymes, when compared to normal fibroblast or tumor cells, that would account for their elevated binding observed *in vivo*.

Evidence to support this conclusion was obtained in experiments which examined the binding of ^{14}C-Misonidazole to mouse liver, spleen, heart, kidney, brain and tumor tissue cubes under controlled oxygen conditions. The results of these studies showed that the K_m value for half-maximal binding and the absolute rates (grains/100 μm^2) observed

for liver were not significantly different from those of other tissues such as brain or heart. These results support the findings obtained with isolated liver cells in that it suggests that liver does not possess a unique complement of nitroreductase enzymes when compared to other normal tissues. Based on these findings, it is likely that the elevated *in vivo* binding observed to liver is due to the organ existing in a reduced state of oxygenation when compared to other normal tissues.

Finally, an evaluation of the sensitizer adduct technique showed that this method has the potential to be a sensitive and reliable method for the determination of *in vivo* pO_2 levels, and that standard pO_2 curves can be generated for most normal tissues. Measurements of the pO_2 of liver using this technique supported the conclusion that liver exists at a relatively low pO_2 *in vivo*.

ACKNOWLEDGEMENT

The development of this project was made possible through the contributions of many people who willingly shared their time and technical knowledge. I would especially like to thank my supervisor, Dr. J.D. Chapman, for providing me with the opportunity to train in the Radiobiology Program and attend several scientific meetings. His ideas, encouragement, and enthusiastic approach to research were a constant source of inspiration.

Dr. Cam Koch generously provided his time and expertise in helping with the oxygen measurements, as well as contributing many helpful suggestions during the course of the project. Dr. Randy Jirtle, of the Department of Radiology, Duke University, provided invaluable assistance with setting up the procedure for the isolation of mouse hepatocytes. I would also like to thank Bert Meeker, Jane Lee, Bonnie Garrecht and Janet Sharplin, who provided much-appreciated assistance with various technical aspects of the project. Special thanks are extended to Jan Steele, who did the histological sectioning of tissues for autoradiography.

I would like to thank K. Liesner, J. Spicer and F. LoCicero of the Audiovisual Department at the Cross Cancer Institute for their preparation of many graphs and slides. I am especially grateful to Miss Karen Brown for typing the manuscript. I would also like to thank Dr. Jerry Miller for his photographic assistance, and Dr. Allan Franko for his advice and encouragement.

These studies were supported by the Alberta Cancer Board and a scholarship awarded by the Natural Sciences and Engineering Council of Canada.

TABLE OF CONTENTS

CHAPTER		PAGE
1.	INTRODUCTION	1
2.	MATERIALS AND METHODS	14
	SECTION I. BINDING OF ^{14}C-MISONIDAZOLE TO CELL SUSPENSIONS IN VITRO	
	Cell Culture	14
	Mouse Hepatocyte Isolation	14
	Drugs	19
	^{14}C-Misonidazole Binding	20
	Calculation of Binding Rate	21
	SECTION II. BINDING OF ^{14}C-MISONIDAZOLE TO MOUSE TISSUE CUBES IN VITRO	
	^{14}C-Misonidazole Binding	22
	Histological Processing	24
	Autoradiographic Techniques	24
	Scoring of Grains	25
	SECTION III. BINDING OF ^{14}C-MISONIDAZOLE TO MOUSE TISSUES IN VIVO	
	Tumor Line and Induction	26
	Binding of ^{14}C-Misonidazole	26
	Drug Injection	27
	Liquid Scintillation Counting	27
	Quench Correction Curve	28

CHAPTER PAGE

3. RESULTS AND DISCUSSION 31

Binding of ^{14}C-Misonidazole to Cell Suspensions *in vitro* 31

4. RESULTS AND DISCUSSION 40

Binding of ^{14}C-Misonidazole to Mouse Tissue Cubes *in vitro* 40

5. RESULTS AND DISCUSSION 63

Binding of ^{14}C-Misonidazole to Mouse Tissues *in vivo* 63

6. GENERAL DISCUSSION AND CONCLUSIONS 70

BIBLIOGRAPHY 77

VITA 83

LIST OF TABLES

TABLE	DESCRIPTION	PAGE
1.	Average Binding Rate of ^{14}C-Misonidazole to Cells at 37°C in Nitrogen	38
2.	K_m Values for Mouse Tissues Estimated from pO_2 Curve	47
3.	Average Grain Density/1200 μm^2 Area for Mouse Tissues Labelled *in vivo* with 50 µM ^{14}C-Misonidazole	64
4.	Average dpm/100 mg (X 10^4) for Mouse Tissues Labelled *in vivo* with 50 µM ^{14}C-Misonidazole	65
5.	Estimated pO_2 Levels for Mouse Brain, Liver and EMT-6 Tumor	67

LIST OF FIGURES

FIGURE	DESCRIPTION	PAGE
1	Proposed Reduction Scheme for Misonidazole	10
2	Quench Correction Curve (Efficiency vs. H#)	30
3	The Binding of ^{14}C-Misonidazole to Mouse Hepatocytes at 37°C	32
4	The Binding of ^{14}C-Misonidazole to Mouse Hepatoma Cells at 37°C.	33
5	The Rate of ^{14}C-Misonidazole Binding to V79 Cells in Nitrogen vs. Drug Concentration	34
6	The Rate of ^{14}C-Misonidazole Binding to EMT-6 Cells in Nitrogen vs. Drug Concentration	35
7	The Rate of ^{14}C-Misonidazole Binding to Mouse Hepatocytes and Hepatoma Cells in Nitrogen vs. Drug Concentration	36
8	The Rate of ^{14}C-Misonidazole Binding to Mouse Liver vs. Tissue pO_2	41
9	The Rate of ^{14}C-Misonidazole Binding to Mouse Brain vs. Tissue pO_2	42
10	The Rate of ^{14}C-Misonidazole Binding to Mouse Heart vs. Tissue pO_2	43
11	The Rate of ^{14}C-Misonidazole Binding to EMT-6 Tumor vs. Tissue pO_2	44
12	The Rate of ^{14}C-Misonidazole Binding to Mouse Kidney vs. Tissue pO_2	45
13	The Rate of ^{14}C-Misonidazole Binding to Mouse Spleen vs. Tissue pO_2	46
14	Grain Density Over Liver Tissue vs. Distance From Tissue Surface	61

LIST OF PLATES

PLATE	DESCRIPTION	PAGE
1	Apparatus used for mouse liver perfusion	18
2	Perfused mouse with blanched liver	18
3	Aluminum chambers used for degassing of tissue cubes	23
4	Grain density at surface of mouse liver cube incubated in nitrogen	50
5	Grain density at surface of mouse liver cube incubated in 30% oxygen	50
6	Grain density at surface of mouse brain cube incubated in nitrogen	52
7	Grain density at surface of mouse brain cube incubated in 30% oxygen	52
8	Grain density at surface of mouse heart cube incubated in nitrogen	54
9	Grain density at surface of mouse heart cube incubated in 30% oxygen	54
10	Grain density at surface of EMT-6 tumor cube incubated in nitrogen	56
11	Grain density at surface of EMT-6 tumor cube incubated in 30% oxygen	56
12	Grain density at surface of mouse kidney cube incubated in nitrogen	58
13	Grain density at surface of mouse kidney cube incubated in 30% oxygen	58
14	Grain density at surface of mouse spleen cube incubated in nitrogen	60
15	Grain density at surface of mouse spleen cube incubated in 30% oxygen	60

CHAPTER 1

INTRODUCTION

The importance of molecular oxygen for the existence of living organisms was recognized long before its actual discovery. As early as 545 B.C. Anaximenes proposed the concept of "pneuma", which was taken up by living bodies during breathing (1). It has since been interpreted that "pneuma" represented early endeavors to elucidate the role of oxygen in living processes. In 1669, John Mayow observed that the survival of a mouse which had been placed under a glass bell, was shortened by the simultaneous presence of a burning candle (2). From his observations, Mayow concluded that the room air was composed of two gases, one which was not used in either combustion or respiration, and a second, which he termed "nitro-aereal" spirit, that could support both processes (2). In 1772, Joseph Priestly discovered a new gas, which was referred to as "dephlogisticated" (oxygenated) air (2). It was not until 1780, however, that Lavoisier demonstrated the process of oxidation and renamed Priestly's gas "oxygen", meaning 'acid-producer' (2).

Biochemically, oxygen plays a vital role in the metabolism and cellular energetics of living organisms. In a complex organism such as man, individual cells rely on the circulatory system to provide both a constant supply of oxygen for the generation of energy and adequate removal of waste products such as carbon dioxide (CO_2). In the absence of oxygen, certain organs, such as smooth and skeletal muscle can

continue to function anaerobically for short periods of time. More sensitive organs, however, such as the brain and heart, cannot function without a constant oxygen supply.

The most important source of energy for the cell is adenosine triphosphate (ATP), a nucleotide consisting of an adenine, a ribose and a triphosphate unit (3). ATP is an 'energy-rich' molecule because its triphosphate unit contains two phosphoanhydride bonds (3). When ATP is hydrolyzed to either adenosine diphosphate (ADP) or adenosine monophosphate (AMP) the energy liberated from the hydrolyzed anhydride bond is used to do 'biological work' such as muscle contraction, active transport of molecules and ions, and the synthesis of macromolecules from simple precursors (3). Thus, the overall goal of energy metabolism is the continual generation of ATP, a process in which molecular oxygen is a vital component.

The generation of ATP within the cell occurs in three major metabolic pathways. Glycolysis, is the sequence of reactions that converts glucose into pyruvate with the net production of 2 molecules of ATP and 1 molecule of nicotinamide adenine dinucleotide (NADH) (4). When oxygen is available, the next stage in the breakdown of glucose is the oxidative decarboxylation of pyruvate to form acetyl coenzyme A (acetyl Co A). The acetyl Co A unit enters a series of reactions known as the tricarboxylic acid cycle, where it is completely oxidized to CO_2 (4). The overall result of this oxidation is the production of 4 pairs of hydrogen atoms (reducing equivalents) in the form of 3 NADH molecules and 1 $FADH_2$ molecule (flavin adenine dinucleotide) (4).

The NADH and $FADH_2$ produced in glycolysis and the citric acid cycle are rich in potential energy due to the high transfer potential

of the electron pair contained in each molecule. In oxidative phosphorylation, these electrons are transferred by a series of electron carriers from NADH and $FADH_2$ to molecular oxygen to form H_2O, a process which results in the generation of ATP (4). Molecular oxygen acts as the ideal electron acceptor because of its high affinity for the H^+ ion and its associated electrons (5). This affinity results in strong binding of the H^+ ion in the water molecule, allowing the liberation of large quantities of energy (5).

The complete combustion of 1 mol glucose results in the net production of 36 mol ATP (4). This process is dependent on the availability of large amounts of oxygen. The combustion of 1 mol glucose consumes 6 mol oxygen, which is the amount of oxygen contained in 130 l of pure oxygen gas or in 650 litres of air (5). If an insufficient amount of oxygen is available, such as in an actively contracting muscle, a small amount of ATP (2 mol) can be produced by glycolysis alone as glucose is broken down to lactate (3). When compared to the amount of ATP produced by the complete combustion of glucose when oxygen is present, it is evident that without an adequate supply of oxygen the energy needs of an organism would not be met.

With the demands of oxidative metabolism, the question arises as to how the body deals with the problem of transporting sufficient oxygen from the external environment to the tissues at a cellular level. This transfer of oxygen from the air to the cells involves a series of steps: 1) the inhalation of air into an external gas exchanger (lungs); 2) diffusion of oxygen into the blood; 3) flow of blood to the tissue; 4) diffusion of oxygen to the cells (5). To ensure that oxygen containing blood is distributed to the cells where it is

needed, a circulatory system has been developed that can be divided into 4 major components: 1) pump: heart, 2) distributing vessels: arteries, 3) exchange vessels: capillaries, 4) collecting vessels: veins.

The circulatory system is composed of two major loops. The pulmonary circulation begins in the right ventricle of the heart and ends in the left atrium after passage through pulmonary arteries (carry blood away from the heart), capillaries (where reoxygenation takes place in the lungs) and pulmonary veins (carry oxygenated blood back to the heart) (5). The systemic circulation, which distributes oxygen rich blood to the organs, begins in the left ventricle which pumps the blood into the aorta and to the organs via numerous arteries. Blood depleted of oxygen is transported back to the right atrium through the systemic veins. The arteries that arise from the aorta form a series of smaller branches called arterioles. The arterioles branch further to form numerous small, thin-walled vessels called capillaries, which have a diameter close to that of red blood cells (5).

The transfer of oxygen from the blood to the tissues occurs in a microvascular unit which is made up of a network of capillaries. Studies of sections of skeletal muscle suggest that the microvascular unit is composed of 240,000 capillaries per square centimeter (5). Capillaries are somewhat more permeable than the plasma membrane of the cells. Oxygen can easily diffuse through the capillary walls into the tissue where it is absorbed by the cells, while carbon dioxide, nitrogenous wastes and other by-products of metabolism diffuse out of the tissue into the blood. Oxygen depleted blood (pO_2 40 mm Hg) leaves

the capillary bed via small venules which drain into the veins that carry the blood back to the heart for reoxygenation (5).

The problem of how to transport sufficient quantities of oxygen in the blood to meet tissue demands has been met by the development of an oxygen carrier. If the blood was composed of a simple aqueous solution, one litre would contain only 3 ml of oxygen since oxygen is poorly soluble in water (5). To increase the carrying capacity of the blood and thereby reduce the blood flow required to supply the cells, 30% of the red blood cell is composed of hemoglobin (Hb), an iron-containing protein molecule which binds oxygen (6). Since each molecule of Hb can bind 4 molecules of oxygen, this increases the carrying capacity of the blood by a factor of 30 over a simple aqueous solution (6). The release of oxygen from hemoglobin is affected by CO_2 which offers an advantage for the discharge of oxygen in tissues. As CO_2 generated by the Krebs cycle is taken up by the blood, the oxygen affinity of the blood falls, thus discharging a greater amount of oxygen to the tissue. This effect, which is also affected by pH, is known as the Bohr Effect.

When the rate of oxygen supply to the tissues is insufficient to meet its metabolic requirements, tissue hypoxia occurs, a condition that causes altered biochemical and physiological function and is a very common and serious aspect of many disease processes. Tissue hypoxia can occur as a result of several factors: 1) reduction in blood flow e.g. cardiogenic, haemorrhagic shock; 2) reduction in arterial oxygen content e.g. ventilatory failure; and 3) reduction in arterial oxygen carrying capacity e.g. severe anaemia or altered haemoglobin (2).

The importance of hypoxia as a problem in the treatment of solid tumors with radiotherapy is well documented in experimental systems. Solid tumors have been shown to contain regions of necrosis and severe vascular insufficiency, and it is in these areas that poorly oxygenated (hypoxic) but viable cells are located (7). Studies have shown that hypoxia renders cells less sensitive to the cytotoxic effects of radiation, while oxygenated cells are 2.5 - 3 X more sensitive (8). This radiobiological effect has implications for cancer therapy in that radioresistant hypoxic cells may survive treatment with radiation and subsequently become reoxygenated and repopulate the tumor. In 1963 Powers and Tolmach demonstrated that in a transplanted neoplasm in rodents, hypoxic cells constitute 10 - 20% (and occasionally over half) of the total viable cell population (9). Evidence also suggests that these cells are a factor in the radiotherapy of human neoplasms as well. This evidence includes the measurement of low oxygen tensions with electrodes, improvement in local control in some hyperbaric oxygen trials and histologies suggestive of hypoxic areas (7).

Many treatment modalities and regimens have been tested in an attempt to solve the problem of tumor hypoxia. A variety of fractionated irradiation schedules have been devised in attempts to maximize cell killing (10). Efforts to improve tumor oxygenation have involved the use of oxygenated perfluorochemical emulsions and hyperbaric oxygen treatment (11,12). Other adjuncts to radiotherapy include hypoxic cell sensitizers (13), as well as agents selectively toxic to hypoxic cells such as hyperthermia and bioreductive alkylating agents (14,7).

The oxygen status of both normal and tumor tissue is an important factor in disease processes, and numerous attempts have been made to devise methods for the accurate determination of tissue oxygen tension. Information about the extent and distribution of hypoxic cells throughout individual tumors, for example, would be useful to the oncologist in designing treatment strategy for a particular tumor. Earlier methods for the study of normal tissue oxygenation involved the introduction of bubbles of inert gas into various organs (15). After the bubbles had equilibrated with the pO_2 of the surrounding tissue they were withdrawn and analyzed. A further modification of this procedure involved introducing gas-filled, open-ended microcapillaries into organs and analyzing the gas in the capillaries after equilibration had been achieved (15).

More recent attempts to determine the oxygen tension in tissues have involved the use of the polarographic electrode. The oxygen electrode was initially developed by Daniel in 1897, and was later applied to tissue studies in 1942 by Davies and Brink (15). These early electrodes were subject to technical limitations which had substantial effects on the current reading obtained, raising questions as to the accuracy of the results. These factors include variations in the diffusion coefficient of oxygen in different tissues; the effect of movement of tissue fluid near the electrode tip; and the poisoning effect of foreign materials (e.g. thiols) which may form complexes with the electrode metal (15).

Since its initial development, there have been considerable variations in the design of oxygen electrodes in an effort to eliminate some of the many problems associated with the system. The recessed

electrode, which was developed by Davies and Brink in 1942, produced absolute readings despite the diffusion conditions in the tissue and also proved to be immune to the poisoning effects of foreign substances (15). The disadvantages that have arisen with this electrode are that its large size prevents measurements from being made continuously and that it responds slowly to changes in pO_2. As a result, this type of electrode has proven useful for intermittent measurements at the tissue surface rather than internally.

A second type of electrode which has been developed for use in tissues is the open electrode (15). Unlike the recessed electrode, the open electrode is suitable for continuous measurements and exhibits a rapid response to variations in oxygen tension (15). There are several disadvantages, however, in that the current output is affected by stirring and differing diffusion coefficients of oxygen in differing parts of the tissue (15). A further problem with open electrodes is that they consume oxygen, a problem in that it affects the conditions that the electrode is attempting to measure.

A development from the open electrode is the ultra-micro needle electrode. This electrode, developed by Cater and Silver in 1961 has a cathode surface of 1 - 5 μm^2. Electrodes of this size present several advantages over larger electrodes in that they cause minimal damage to tissues in which they are inserted; consume very small amounts of oxygen; exhibit a rapid response and are relatively insensitive to the effects of stirring. The small size does pose some problems, however, in that these electrodes are easily damaged and are subject to protein deposition (15). While modern microelectrodes could prove potentially

useful in defining the hypoxic state of individual human cancers, the technique is limited for clinical use because it is invasive and the implantation of the electrode can introduce oxygen and yield false measurements.

One very promising development in the search for a means to detect and determine the hypoxic fraction in human tumors is the use of radiosensitizer adducts as markers for hypoxic cells. Several nitro-aromatic drugs, such as Misonidazole (MISO) have been shown to selectively sensitize resistant hypoxic mammalian cells to radiation (16,17). With the exception of a head and neck trial reported by Overgaard, the results of clinical trials have shown no significant improvements in tumor responses and/or cures from patients treated with MISO and radiation (18). Further in vitro studies with Carbon-14 (^{14}C)-MISO (labelled in the 2-carbon position) showed that adducts of labelled drug become bound to the acid insoluble fractions of hypoxic mammalian cells (51). This process was shown to be 20 - 50 X more efficient in the absence of oxygen than in aerobic cells (51). The proposed scheme for the reduction of MISO to an activated species which can bind to hypoxic cells is outlined in Figure 1 (19). Further studies showed that when cells labelled with ^{14}C-MISO under hypoxic conditions were made to proliferate under aerobic conditions in petri dishes, the ^{14}C-MISO adducts were released from the cells with a half-life of 50 - 55 hours (50). These findings suggested that sensitizer adducts could be useful as markers for hypoxic cells in solid tumors.

In additional studies, ^{14}C-MISO was shown to label zones within multicellular spheroids and EMT-6 tumors growing in Balb/C mice (20).

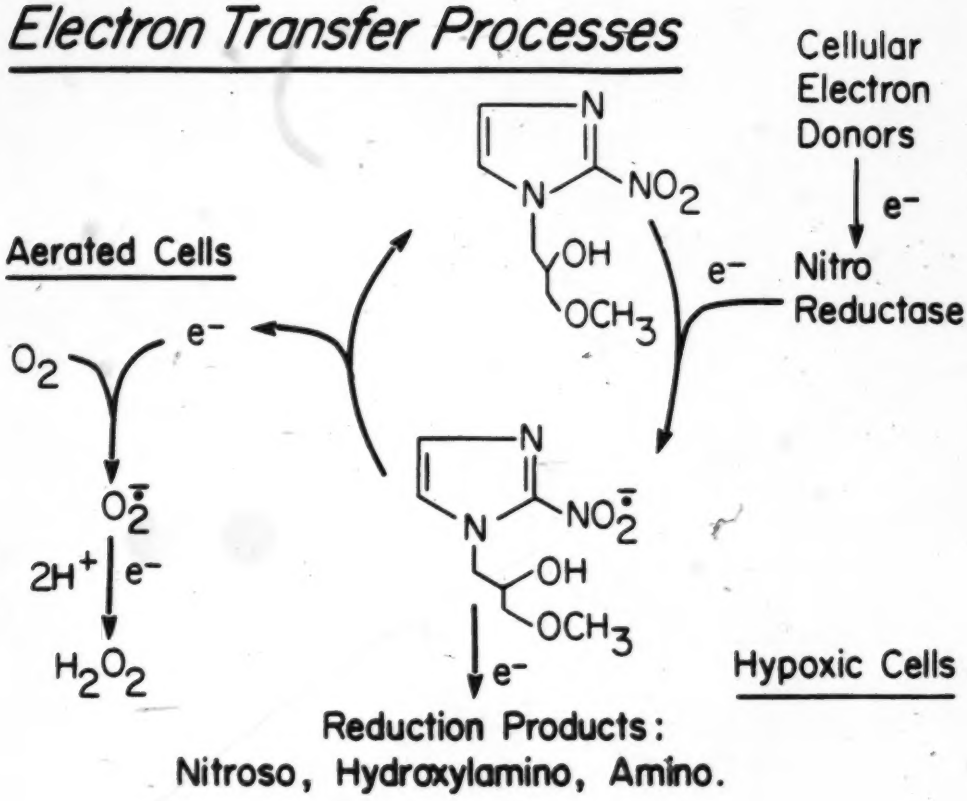

FIGURE 1: Proposed reduction scheme for Misonidazole

In these studies, ^{14}C-MISO labelled tissue was visualized by autoradiography of histological sections, and was postulated to coincide with viable hypoxic cells (20). Further studies with multicellular spheroids indicated that the zone of labelling was consistent with the hypoxic fraction of spheroids computed by oxygen diffusion and consumption criteria.

Studies by Garrecht and Chapman (21) were designed to determine if hypoxic tissues in animals selectively bind ^{14}C-MISO and, if at times adequate for clearance and excretion of unbound drug, large tumor/tissue ratios of ^{14}C activity could be measured. After multiple drug injections it was determined using both autoradiographic and scintillation procedures that the level of ^{14}C retained in the tumor was 2 - 15 times higher than that retained in all other normal tissues except liver (21). The level of ^{14}C-MISO retained in liver was similar to that found in the tumor (21). These studies gave further evidence that hypoxic cell sensitizers tagged with an appropriate label that could be detected by noninvasive techniques could become a clinical marker for hypoxic tumor cells. In addition, hypoxic cell markers could also be used to study questions relating to the reoxygenation of hypoxic tumor cells, and the oxygenation status of cells in non-neoplastic tissues suffering other disease syndromes.

Several other novel techniques have been proposed for detecting and imaging hypoxic cells in tumors, although most of these are still in the developmental stages. Some of these new developments include:

1) Positron Emission Tomography (22)
2) Fluorescent-labelled nitroaromatic drugs as hypoxic cell markers (23)

3) Detection of γ-labelled sensitizer adducts (4-Br MISO) by Single Photon Emission Tomography
4) The measurement of intracellular ^{31}P in ATP molecules by nuclear magnetic resonance technique (24).

The further development of new non-invasive techniques for detection of hypoxia in tumors will have a major impact on treatment strategies in clinical oncology.

The studies described in this thesis were designed to address two areas of interest:

1) To determine if the increased in vivo binding of ^{14}C-MISO to liver observed in the studies by Garrecht and Chapman was due to a) a distinctive enzyme complement associated with drug detoxification, b) to the liver existing at a lower pO_2 than other normal tissues or c) some other factors.
2) To determine if the sensitizer-adduct technique can be developed as a probe for cellular pO_2 in other normal tissues.

Chapter Three describes the results of experiments which examined the aerobic and hypoxic binding rates of ^{14}C-MISO to freshly isolated mouse hepatocytes, mouse hepatoma cells, V79 Chinese hamster fibroblasts and EMT-6 fibrosarcoma mouse cells. Chapter Four presents the results of labelling experiments with mouse tissue cubes in vitro. Using autoradiographic techniques, binding curves were obtained for mouse liver, spleen, heart, kidney, brain and EMT-6 tumor as a function of pO_2. The implications of the results obtained in Chapter's 3 and 4 in terms of liver oxygenation are described. In Chapter Five, the binding of ^{14}C-MISO to mouse tissues in vivo is quantified using autoradiographic and scintillation procedures. The standard curves are

utilized in an attempt to determine the cellular oxygen concentration in selected mouse tissues in vivo. The data is expressed as both the % oxygen in the gas phase in equilibrium with the tissue (i.e. pO_2) and as mm Hg.

CHAPTER 2

MATERIALS AND METHODS

SECTION I. BINDING OF ^{14}C-MISONIDAZOLE TO CELL SUSPENSIONS IN VITRO

CELL CULTURE

Mouse hepatoma 129P cells were generously supplied by Dr. Allan Paterson, Department of Pharmacology, University of Alberta. Hepatoma cells were cultured in suspension in 100 ml bottles (GIBCO) and transferred twice weekly. Cells were grown in Spinner Minimal Essential Medium (MEM) (GIBCO) containing 5% horse serum (Flow Laboratories), 2% MEM non-essential amino acid (50X concentration), 2% glutamine, and 1% penicillin - streptomycin (GIBCO). For cell transfer, approximately 2 x 10^5 cells were added to 20 ml Spinner MEM.

V79 Chinese hamster lung fibroblasts and EMT-6 fibrosarcoma mouse tumor cells were cultured as monolayers on 25 cm^2 tissue culture flasks (Corning). Confluent cells were trypsinized and transferred twice weekly in Standard Minimal Essential Medium (GIBCO) or Waymouth's Medium containing 5% fetal calf serum (GIBCO), respectively. Approximately 5 x 10^5 cells were added to each flask for cell transfer. All cell cultures were incubated at 37°C in a humidified atmosphere of 5% CO_2 in air.

MOUSE HEPATOCYTE ISOLATION

INTRODUCTION

It is well established that isolated intact mammalian hepatocytes

represent a useful system for the study of hepatic metabolism (30-45). During the past 20 years a number of different procedures have been developed for the isolation of hepatocytes. These include non-perfusion techniques such as digestion of liver pieces in tetraphenylboron, a K^+-chelator (25) and the use of enzymes such as trypsin (26,27) or a mixture of collagenase and hyaluronidase (28,29) as dissociating agents.

A more widely used procedure is the two-step in situ collagenase perfusion method, originally introduced by Berry and Friend (30) and subsequently modified by numerous other investigators (31-39). Various factors, including the concentration of collagenase in the perfusate, the method of hepatocyte dispersal after perfusion, the force of isolated cell pelleting, the rate of perfusion, and the composition of the perfusate media, have been shown to influence the yield and viability of isolated hepatocytes. In the perfusion technique, the perfusate is pumped through vascular pathways, resulting in dissociated liver tissue that can be further dispersed into isolated cells by simple mechanical means. Hepatocytes isolated by this method have been successfully cultured in both suspension and conventional monolayer (40-47). The mouse hepatocytes used in the ^{14}C-Misonidazole (^{14}C-MISO) binding studies described in this thesis were isolated using the collagenase perfusion technique developed by Berry and Friend (30) and modified by Deschenes et al. (48,49).

ANIMALS

Female Balb/C mice were supplied by the Small Animal Breeding Unit of the University of Alberta. Mice were housed at a maximum of 5

animals per cage, fed Rodent Chow (Ralston Purina Co.) and water ad libitum, and maintained on a 12 hour light/dark cycle. Animals weighed 19-23 g at the time of experimentation.

SURGICAL PROCEDURE

Prior to commencing surgery, the donor mouse was anesthetized with an intraperitoneal injection of Tribromoethanol. A Tuberculin 1 ml syringe (Becton-Dickinson) and a 26 gauge 1/2" needle (Yale) were used for injection. The animal was securely pinned to a styrofoam tray and a midline incision was made to expose the abdominal cavity. Non-absorbable silk suture (3-0) (Davis-Creek) was used to securely ligate both renal veins. The abdominal branch of the inferior vena cava was clamped with a hemostat below the level of the renal veins. A loose suture was tied around the inferior vena cava just above the hemostat. During the procedure the abdominal cavity was kept moist and clear of blood by flushing the region with physiological saline. The inferior vena cava was cannulated above the level of the renal veins with a 20 gauge Quik-Cath teflon catheter and the loose suture tightened to fasten it firmly in place. The peristaltic pump (Plate 1) was turned on to begin perfusion of the liver with 50 ml calcium-free buffer at a rate of 5 ml/min. The portal vein was cut to allow drainage of the perfusate which was not recirculated. The diaphragm was then cut to expose the thoracic branch of the inferior vena cava which was clamped with a hemostat.

One litre of calcium-free buffer contained 0.5 g potassium chloride (J.T. Baker Chemical Co.), 8.3 g sodium chloride (A. & C.

PLATE 1

Apparatus used for mouse liver perfusion

PLATE 2

Perfused mouse with blanched liver.

American Chemicals) and 2.4 g 4-(2-hydroxyethyl)-1-piperazineethane-sulfonic acid buffer (HEPES) (Grand Island Biological Co.). The pH of the buffer was adjusted to 7.4 with sodium hydroxide. After conclusion of the initial perfusion, the buffer was changed to one of identical composition with the addition of calcium chloride ($CaCl_2 \cdot 2H_2O$) at a concentration of 74 mg/litre and collagenase (Type IV, Sigma Chemical Company) at a concentration of 0.5 mg/ml of buffer. The liver was perfused with 50 ml of the collagenase solution at a rate of 5 ml/min. All buffer solutions were maintained at 37°C in a water bath during the perfusion.

At the end of the perfusion, the completely blanched liver pieces (Plate 2) were removed and placed in a sterile beaker containing 30 ml of calcium-free buffer. The liver pieces were minced with scissors and the resultant material was filtered through a Nitex nylon mesh filter (100 µm pore size, TETKO) to remove cell clumps and debris. The cell suspension was washed in ice-cold calcium-free buffer and centrifuged for 2 min at 50 g (700 rpm). This washing procedure was repeated twice. The total cell yield obtained by this procedure was approximately 5 x 10^7 cells/liver. A Trypan blue exclusion viability test indicated that 95 - 98% of the isolated hepatocytes excluded the dye.

DRUGS

^{14}C-MISO (1-(2-nitro-1-imidazole)-3-methoxy-2-propanol) labelled at C-2 of the imidazole ring was generously provided by Dr. W.E. Scott of Hoffman - La Roche (Nutley, N.J.). The specific activity was 230 µCi/mg. ^{14}C-MISO at a specific activity of 86 µCi/mg and 90 µCi/mg was

purchased from SRI (Stanford Research Institute, Palo Alto, California).

^{14}C-MISONIDAZOLE BINDING

^{14}C-MISO binding to different cell types was determined using the procedure described by Chapman (50,51). Chinese hamster V79 fibroblasts, EMT-6 fibrosarcoma mouse tumor cells, freshly isolated mouse hepatocytes or mouse hepatoma cells, were suspended in Spinner MEM (Mg^{2+} and Ca^{2+} free) plus 10% fetal calf serum, and the cell concentration adjusted to 5×10^6 cells/ml. Six millilitres of the cell suspension were transferred to glass spinner flasks specially designed to allow control of the oxygen levels in the gas phase (52). The temperature of the cell suspension was maintained at 37°C by suspending the chambers in a heated water bath. For aerobic conditions cells were gassed with a humidified gas mixture of 5% CO_2 plus air at a flow rate of 1/2 litre/min. To achieve hypoxia the cells were degassed with a gas mixture of 5% CO_2 plus 95% ultrapure nitrogen at a flow rate of 1 litre/min. Following a 1 hour degassing period, ^{14}C-MISO (specific activity 86 µCi/mg) was added to the chambers to achieve a drug concentration of either 10, 50, 100, 200 or 1000 µM.

At various times following drug addition, 0.1 ml samples of the cell suspension were removed through the sampling port in the chamber and added to 1.5 ml 5% cold trichloracetic acid (TCA) to precipitate the macromolecular fraction. Samples were kept on ice for 15-20 minutes and filtered through Whatman Glass Microfibre filters (2-5 cm) (Fisher Scientific) using a Millipore filter. The filters were washed twice

with cold 5% TCA, placed in glass scintillation vials (Fisher Scientific) and dried for 2 - 3 hours in an oven maintained at 65°C. 10 ml of scintillation fluid (ScintiVerse I, Fisher Scientific) were added to each vial and the ^{14}C activity was determined using a Beckman LS 7000 Liquid Scintillation Counter (Program 4). The binding rate was calculated and expressed as picomoles of ^{14}C-MISO bound per million cells per hour.

Calculation of Binding Rate - pmoles/10^6 cells/hr

The binding rate was calculated using the following method:

1) Subtract background cpm (control sample)

   Multiply by 2 X (to calculate for 10^6 cells)

2) Convert cpm to dpm - $\text{dpm} = \frac{\text{cpm}}{\text{counting efficiency}}$

   Assume 90% efficiency, therefore $\text{dpm} = \frac{\text{cpm}}{0.90}$

3) Convert dpm to µCi $\mu\text{Ci} = \frac{\text{dpm}}{2.22 \times 10^6 \text{ dpm}/\mu\text{Ci}}$

4) Convert µCi to mg $\text{mg} = \frac{\mu\text{Ci}}{\text{specific activity of drug}}$

   (i.e. 86 µCi/mg)

5) Convert mg to moles $\text{moles} = \frac{\text{mg}}{\text{Molecular weight of drug}}$ (MW MISO = 201)

   therefore, $\text{moles} = \frac{\text{mg}}{201}$

6) Convert moles to picomoles - 1 picomole = 10^{-12} moles

SECTION II. BINDING OF ^{14}C-MISONIDAZOLE TO MOUSE TISSUE CUBES IN VITRO

^{14}C-MISONIDAZOLE BINDING

Female Balb/C mice weighing 20 - 25 g were used for all experiments. The donor mouse was killed by cervical dislocation and the liver, kidney, heart, spleen, brain or EMT-6 tumor were removed and placed in a sterile petri dish containing 10 ml of Spinner MEM (low bicarbonate, 20 mM HEPES, 10% fetal calf serum and penicillin-streptomycin). The procedure used for EMT-6 tumor implantation is outlined in Section III. Using a sterile razor blade the tissue samples were cut into cubic fragments with sides of 1 - 2 mm. Tissue cubes (10 cubes/dish) were transferred to 50 mm Pyrex petri dishes (Corning) containing 5 ml of Spinner MEM and 50 μM ^{14}C-MISO (specific activity 230 or 86 μCi/mg). One mouse was used in each experiment.

Dishes were placed in specially designed leak-proof aluminum chambers (53) (Plate 3) along with a petri dish filled with distilled water to provide humidity. For chambers gassed with pure nitrogen, the distilled water was replaced with a .1 M solution of sodium carbonate and sodium dithionite, which acts as a reducing agent to scavenge oxygen from the chamber. The chambers were sealed and connected to a manifold. The air in the chambers was replaced with gas containing the desired oxygen concentration by repeated gas exchanges using a vacuum pump and gas mixture (Union Carbide) (73). The manifold, all connections, and the gas pressure regulator were stainless steel. The final oxygen concentration in the chambers ranged from 0.1 - 30% (.76 - 228 mm Hg).

PLATE 3

Aluminum chambers used for degassing of tissue cubes

The sealed chambers were placed on a shaker plate in an environmental chamber at 37°C and shaken at 70 cycles/min. After approximately 30 minutes, the media in the petri dishes had equilibrated at 37°C. It was estimated that by this time the oxygen content of the media was within 20 ppm of the level in the gas phase (54). Incubation was continued for an additional 3 hours after which the actual % oxygen in the gas phase was measured using a modified Clarke Electrode (55).

HISTOLOGICAL PROCESSING

After completion of the incubation period, the dishes were removed and placed on cold metal trays. The tissue cubes were washed 3 X with saline, 2 X with 10% buffered formalin, and then fixed in formalin for 24 hours. Fixed tissue cubes were embedded in wax and 4 µm serial sections were obtained. As a control, 10 µl of the radioactive media in each dish was added to a glass scintillation vial containing 15 ml of Scintillation fluid (ScintiVerse I, Fisher) and the ^{14}C activity determined in a Beckman LS 7000 Liquid Scintillation Counter.

AUTORADIOGRAPHIC TECHNIQUES

Dehydrated histological sections were dewaxed prior to autoradiography and stored at 4°C in distilled water. The technique used for autoradiography is a modification of the procedure outlined by Rogers (56). NTB-2 Liquid Nuclear Track Emulsion (Kodak) was melted at 45°C, diluted with an equal volume of distilled water, and poured into a plastic dipping pot maintained at 45°C. Dewaxed slides were gently shaken to remove excess water, dipped into the melted emulsion, wiped

and placed on cold metal trays to gel. After 20 minutes, the slides were transferred to glass holders, kept in a light-tight box for 1 1/2 hours, and then dried in silica gel for 2 hours. When dry, the slides were wrapped tightly in cloth and stored in a foil-wrapped can. Excess moisture was prevented from accumulating by placing a silica gel filled petri dish in the bottom of the can. Slides were stored in the refrigerator at 4°C for four to fourteen days. Slides were developed in D19 (Kodak) for 3 minutes, dipped in 3% acetic acid stop bath (Kodak) and fixed for 3 minutes in Kodak fixer. All solutions were maintained at 17°C during the developing procedure. Slides were rinsed in cold running water for 4 minutes, wiped and air dryed for 24 hours before staining with hematoxylin and eosin.

SCORING OF GRAINS

Grains were scored under oil immersion using a 10 x 10 μm grid aligned perpendicular to the edge of the cube. Grains were scored on sections chosen from the center of the tissue cube. The grain density over the outermost cell layer was determined for each oxygen concentration by averaging a large number of single counts and subtracting the mean background grain density.

SECTION III. BINDING OF ^{14}C-MISONIDAZOLE TO MOUSE TISSUES IN VIVO

TUMOR LINE AND INDUCTION

Female Balb/C mice weighing 20 - 25 g were used for all experiments. The tumor line used was the EMT-6 mouse fibrosarcoma, which is maintained in culture by alternate passage in vivo and in vitro. For tumor induction, 2 x 10^6 EMT-6 cells in 0.05 ml Waymouth's medium (GIBCO) were injected subcutaneously in the animal's flank so that a small bubble of cells was visible. A Tuberculin 1 ml syringe (Becton Dickson and Co.) and a 26 gauge 3/8" Yale needle (Becton Dickson and Co.) was used for injection. After 14 days, the tumors grew to about 1 - 2 cm in diameter. Mice with tumors exhibiting signs of surface necrosis were not used in the labelling experiment.

BINDING OF ^{14}C-MISONIDAZOLE

Female Balb/C mice implanted with EMT-6 tumors were injected with 50 μM ^{14}C-MISO (10 μg/gm body weight) and exposed to one of 3 different breathing conditions for a 3 hour period:
Air, 95% O_2 + 5% CO_2 (Carbogen - Medigas) or 8% O_2 + 92% N_2.
During the gassing period the mice were housed in a specially designed plexiglass cage. Three mice were used for each different breathing condition. The gas flow rate was maintained at 1 litre/min. High vacuum grease (Dow Corning) was used to seal the chamber so that no leakage occurred. During the experiment with 92% N_2 the cage was placed on a heating pad kept on a low setting to ensure that the body temperature of the mouse remained constant at 37°C. A rectal thermometer (Tele-Thermometer YSI) was used to periodically monitor the body temperature of the animal.

DRUG INJECTION

^{14}C-MISO with a specific activity of 230 μCi/mg was used for injection. A drug level of 50 μM was maintained during the 3 hour labelling period using the following injection schedule:

time 0	50 μM ^{14}C MISO
time 45 min	25 μM ^{14}C MISO
time 90 min	25 μM ^{14}C MISO
time 135 min	25 μM ^{14}C MISO

Since the half-life of ^{14}C-MISO in mouse plasma is 30 - 40 minutes, the 3 additional injections of 25 μM ensured that the average level of drug in the animal over the labelling period would remain relatively constant at 50 μM. Animals were killed by cervical dislocation approximately 21 hours after injection (to allow clearance of unbound drug from the animal) and the brain, muscle, kidney, heart, liver, spleen and tumor were removed. One-half of each tissue was fixed in 10% buffered formalin, the rest was processed for liquid scintillation counting. Fixed tissues were embedded in wax and 4 μm serial sections were cut. Dewaxed slides were dipped in NTB-2 Nuclear Track Emulsion as described previously and exposed for 14 days. After developing, the slides were stained with hematoxylin and eosin. The distribution of grains over the tissue sections was determined under oil immersion using a 10 x 10 μm ocular grid. Grains were counted in a 1200 μm square area at random places over the tissues. Background grains were subtracted from all counts.

LIQUID SCINTILLATION COUNTING

Tissue samples were minced thoroughly and transferred to pre-

weighed glass scintillation vials. 1 N potassium hydroxide (KOH) was added to each sample (10 parts KOH to 1 part tissue) and the vials were put on an automatic shaker for 2 days to facilitate dissolution of the tissue. After the tissues were completely dissolved, samples were neutralized with an equal volume of 1 N hydrochloric acid (HCl). 200 µl of the neutralized solutions were added to glass scintillation vials containing 15 ml Scinti Verse I. Vials were shaken and the radioactivity counted in a Beckman LS 700 scintillation counter (Program 4). The radioactivity was calculated for each tissue in terms of dpm/100 mg tissue (disintegrations per minute). The counts per minute (cpm) detected by the scintillation counter varies with the counting efficiency of each sample which is determined by quenching due to differences in sample colour. Dpm values were calculated from cpm using the following equation:

$$\text{dpm} = \frac{\text{cpm}}{\text{counting efficiency}}$$

A quench correction curve was used to determine the counting efficiency for each sample.

QUENCH CORRECTION CURVE

A Balb/C mouse was killed by cervical dislocation, and the liver was removed, minced and mixed with blood. The blood-liver mixture was transferred to a 3 ml syringe (Becton Dickson Co.) and pushed through a series of successively smaller needles until a fine paste was obtained. Small amounts of the blood-liver homogenate ranging from .0017 - .07 g were put into preweighed scintillation vials. 1 ml of 1 N KOH was added

to each vial, and the samples were put on an automatic shaker table for digestion. Digested samples were neutralized with 1 ml 1 N HCl. A known amount of radioactivity (4.1×10^4 dpm) in a 20 µl volume was added to each vial. 15 ml Scinti Verse I was added, and the samples were counted on program 4. The counting efficiency, calculated as $\frac{\text{cpm observed}}{\text{dpm added}}$ was plotted on linear graph paper against the corresponding $H^{\#}$ to obtain the quench correction curve shown in Figure 2. The $H^{\#}$ indicates the degree of quenching in a sample and will increase as the amount of quenching increases and the counting efficiency decreases. Specifically, the $H^{\#}$ is the numerical difference between the leading edge of a quenched sample photon energy spectrum and that of an unquenched external λ-emitting standard.

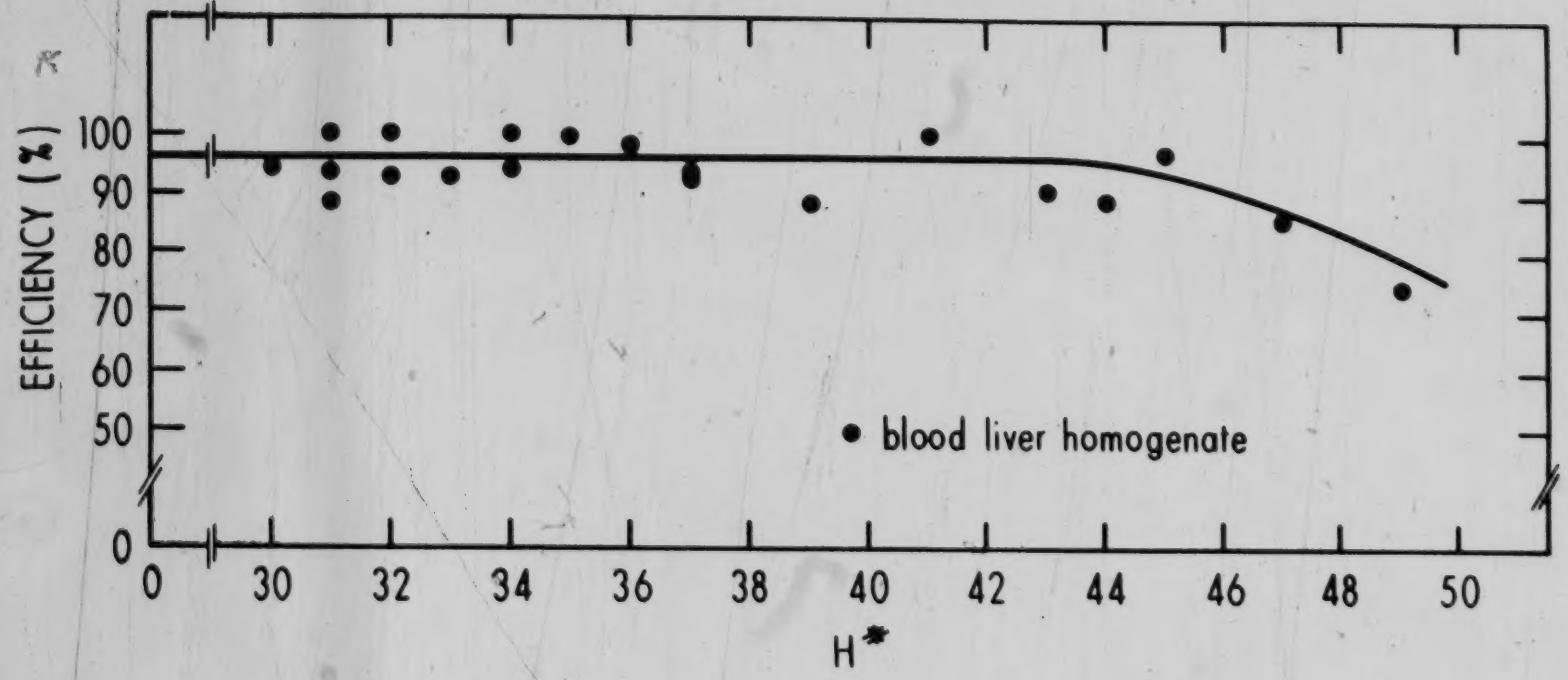

FIGURE 2: Quench curve (efficiency vs. $H^{\#}$).

CHAPTER 3

RESULTS AND DISCUSSION

Binding of ^{14}C-Misonidazole to Cell Suspensions *in vitro*

The uptake of 10 μM ^{14}C-MISO by freshly isolated mouse hepatocytes and mouse hepatoma cells labelled in both hypoxic and aerobic conditions at 37°C is shown in Figures 3 and 4, respectively. No significant time dependent uptake of acid-precipitable counts occurred over a 3 hour period when cells were incubated in aerobic conditions. Under hypoxic conditions, the binding of ^{14}C-MISO to the macromolecular fraction of both hepatocytes and hepatoma cells was a linear function of the incubation time similar to kinetics observed with other cell lines (50). The linear uptake of ^{14}C-MISO observed to hepatocytes was an independent indication that the isolated cells remained viable during the period that binding was being measured. The procedure used for liver cell preparation most likely results in a viable cell population suitable for short-term culture experiments.

Binding studies utilizing a concentration range of 10 - 1000 μM ^{14}C-MISO were performed with mouse hepatocytes, mouse hepatoma cells, EMT-6 tumor cells and V79 Chinese hamster fibroblasts. The results of several independent experiments are presented in Figures 5 - 7. The initial rate of ^{14}C adduct formation for all cell lines is expressed in units of pmoles/10^6 cells/hr. Background counts measured at the 0 time point were subtracted before binding rates were calculated. It can be seen that the initial rate of binding of ^{14}C to the macromolecular fraction of hypoxic cells increases with increasing MISO concentration. This

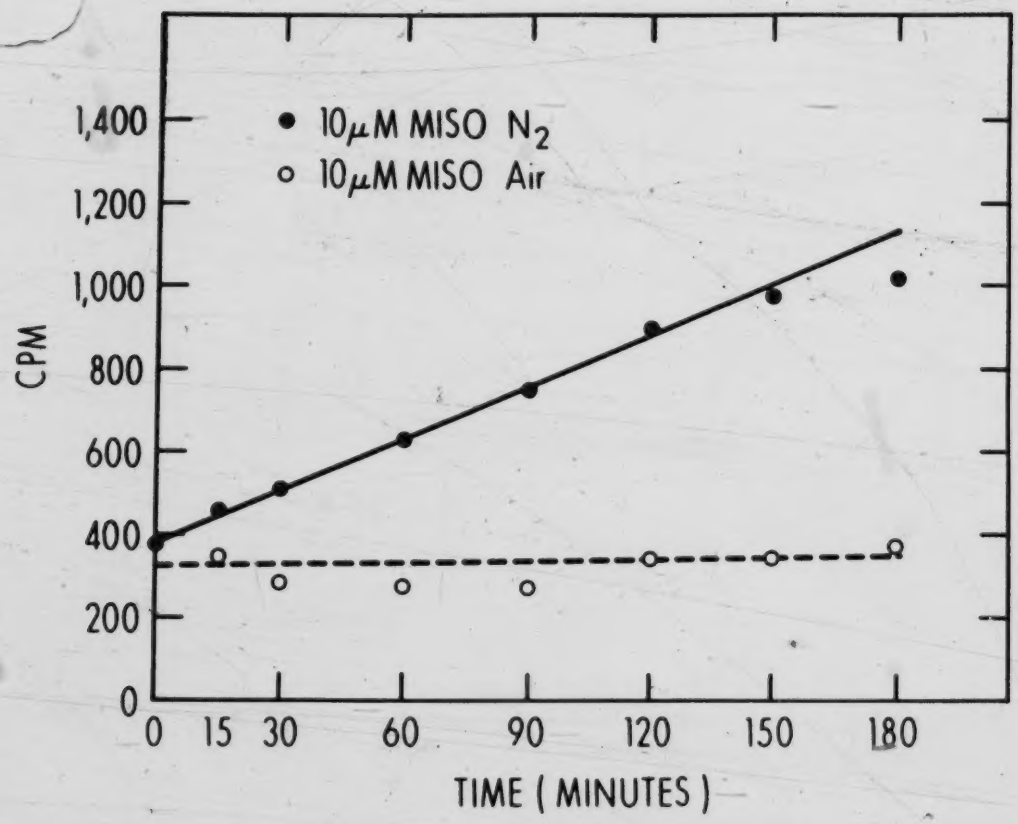

FIGURE 3: The binding of ^{14}C-Misonidazole to mouse hepatocytes at 37°C. Each data point represents the average of two counts.

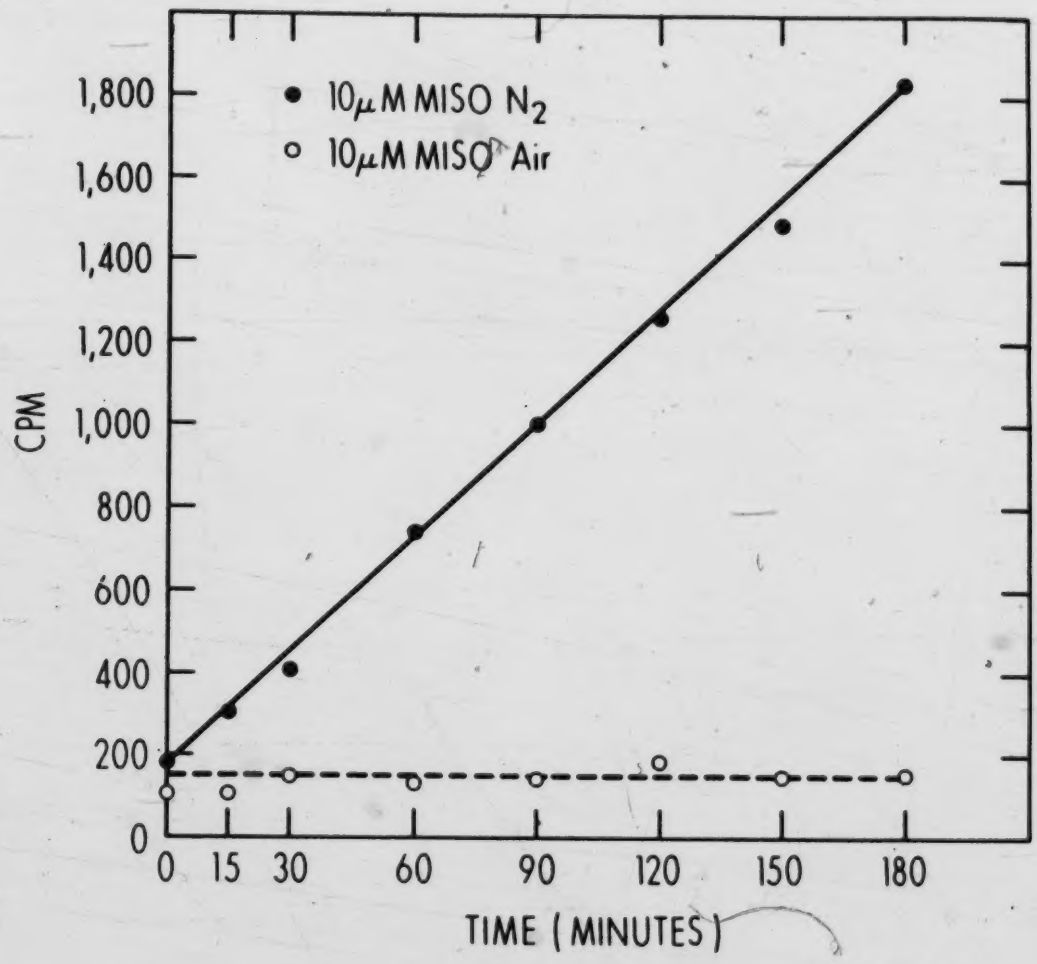

FIGURE 4: The binding of ^{14}C-Misonidazole to mouse hepatoma cells at 37°C. Each data point represents the average of two counts.

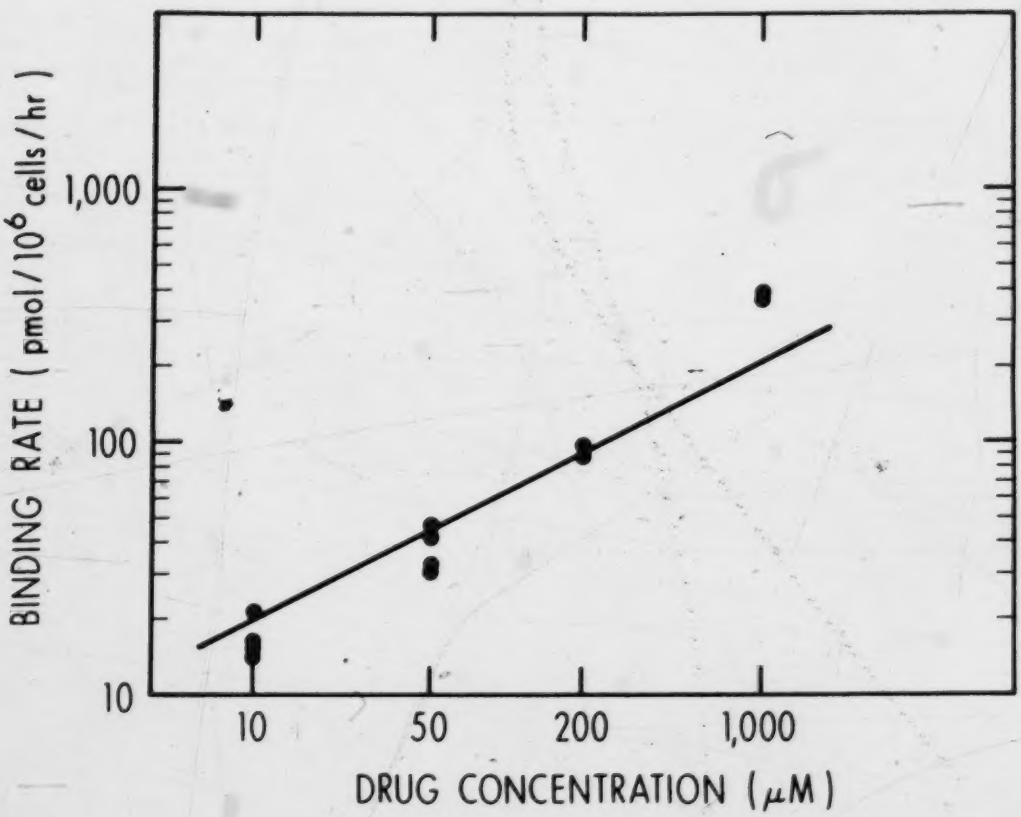

FIGURE 5: The rate of ^{14}C-Misonidazole binding to V79 cells in nitrogen vs. drug concentration.

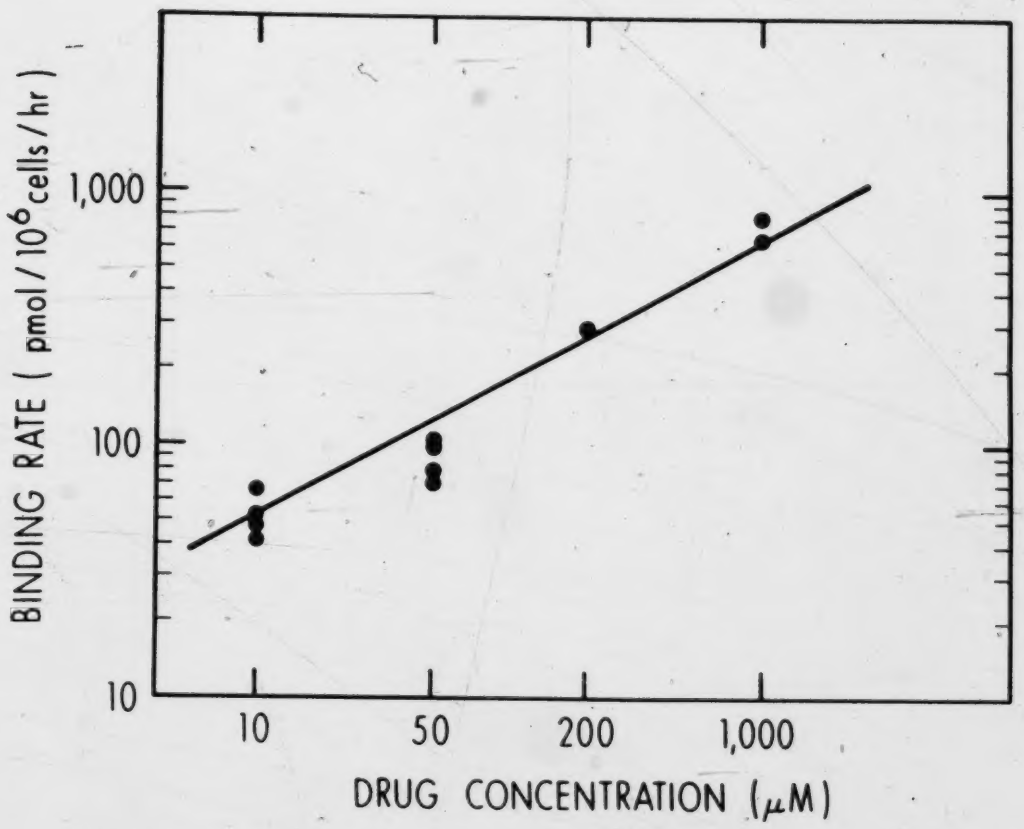

FIGURE 6: The rate of ^{14}C-Misonidazole binding to EMT-6 cells in nitrogen vs. drug concentration.

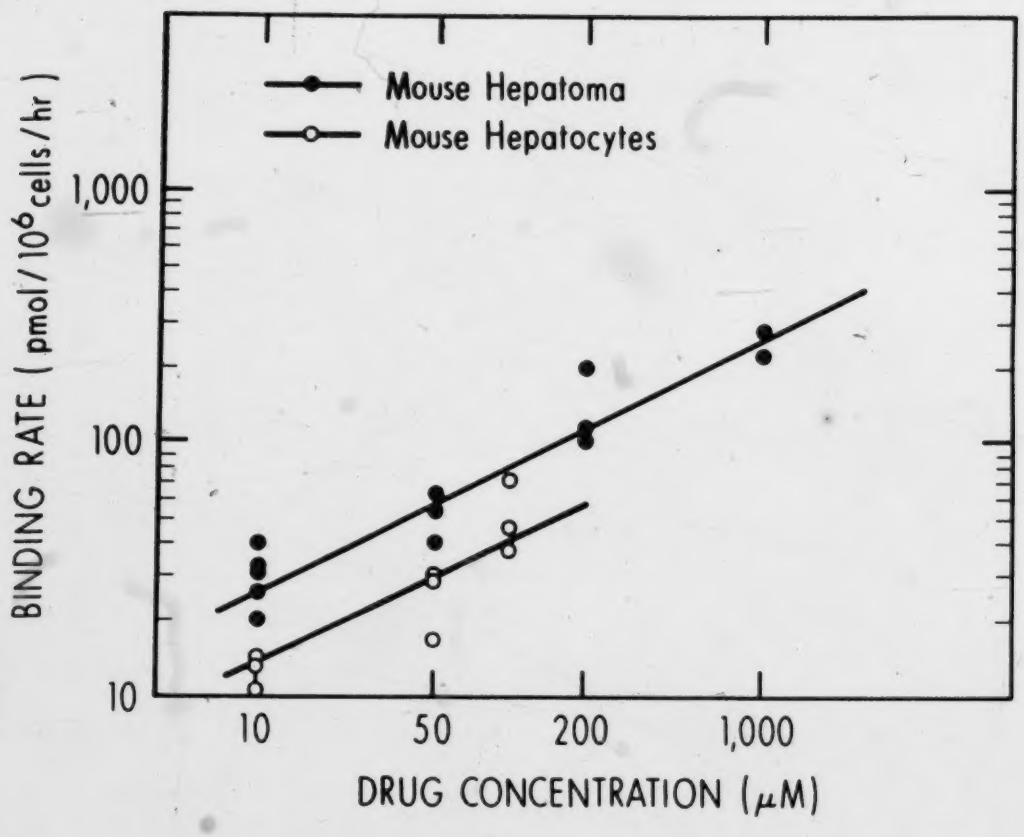

FIGURE 7: The rate of ^{14}C-Misonidazole binding to mouse hepatocytes and hepatoma cells in nitrogen vs. drug concentration.

increase is consistent with half-order kinetics in that the binding rate varies as the square root of the drug concentration.

Table 1 compares the average binding rates of mouse hepatocytes, hepatoma cells, EMT-6 tumor cells and V79 fibroblasts at 10 μM and 50 μM ^{14}C-MISO. On a per cell basis, EMT-6 cells bound the greatest amount of ^{14}C-MISO when compared to the other cell lines. Mouse hepatocytes exhibited the least amount of binding on a per cell basis, 3 - 4 fold less than EMT-6 tumor cells. This difference in binding rate cannot be explained by taking into consideration the relative volumes of the two cell types since by Coulter Counter volume analysis it was determined that EMT-6 cells and mouse hepatocytes are similar in size. V79 cells, which have a cellular volume approximately one-half that of EMT-6 cells, also exhibit greater binding than mouse hepatocytes.

One question which could be raised concerning the low rate of binding observed to mouse hepatocytes, is the possibility that the tissue culture media used to maintain the cells during binding was not adequate in its nutrient content to keep the cells in a fully functional metabolic state. The cells, although viable, may have exhibited a lower rate of binding as a result of some deficiency in a necessary growth factor or hormone. A survey of the literature, however, shows that for short-term culture experiments a standard medium supplemented with serum is sufficient for the cell to express a complete range of biochemical functions (40-47). In long-term culture of hepatocytes using collagen-coated dishes, a progressive decrease in both the number of surviving cells and a reduction in many of the metabolic functions (notably P-450 activity) has been noted within 3 -

TABLE 1

AVERAGE BINDING RATE OF ^{14}C-MISONIDAZOLE TO CELLS AT 37°C IN NITROGEN

CELL TYPE	BINDING RATE (pmoles/10^6 cells/hr) 10 μM	50 μM
EMT-6	51.5 ± 10.8	87.2 ± 14.8
Hepatoma	29.8 ± 7.5	53.6 ± 10.9
V-79	13.5 ± 5.4	37.6 ± 6.1
Hepatocytes	12.3 ± 2.5	25.1 ± 7.6

Standard deviation is shown for all values

5 days (44). To maintain cells for longer periods of time, development of improved media has included both refinements in basal media and the replacement of serum supplements with a variety of hormones, growth factors and trace elements (44). Specifically, this includes the addition of the hormones insulin, glucagon, prolactin and growth hormone as well as epidermal growth factor and trace elements such as copper, selenium and zinc (44). Since the binding experiments with hepatocytes in this study were carried out immediately after the cells were isolated and did not involve long-term culture we have assumed that the media used (Spinner MEM & 10% FCS) was adequate to sustain normal hepatocyte functions over this time. It is unlikely that the low *in vitro* binding rate observed to mouse hepatocytes was due to an immediate decrease in the biochemical activity of the isolated cells.

CHAPTER 4

RESULTS AND DISCUSSION

Binding of ^{14}C-Misonidazole to Mouse Tissue Cubes *in vitro*

In addition to examining the binding of ^{14}C-MISO to individual liver cells *in vitro* the oxygen dependence of binding to liver tissue cubes *in vitro* was also determined. Standard binding curves were determined for mouse liver, spleen, heart, brain, kidney and EMT-6 tumor by plotting the average grain density/100 μm^2 area at the outermost cell layer of the tissue cube vs. the concentration of oxygen in the gas phase. These data are shown in Figures 8 - 13. Each graph shows the results of two and, in the case of liver, three independent experiments. The average grain counts were determined with an ocular grid by averaging at least 100 individual counts for each point and subtracting the background counts obtained over the emulsion. The standard error is shown for each value.

Similar binding patterns were obtained for brain, liver and heart over all oxygen concentrations. Tumor demonstrated a binding pattern similar to liver but in extreme hypoxia tumor exhibited a significantly higher binding rate. This result is not surprising in light of the *in vitro* binding data discussed in Chapter 3. Table 2 shows the K_m values for each tissue. The K_m value is defined as the concentration of oxygen where half-maximal binding is observed. No difference was observed in the K_m values obtained for brain, liver, heart and tumor ($\sim$ .3%). These kinetics would suggest that these tissues *in vivo*, if at the same oxygen tension, would bind the same amount of ^{14}C-MISO. Kidney and spleen had significantly higher K_m values than the other tissues,

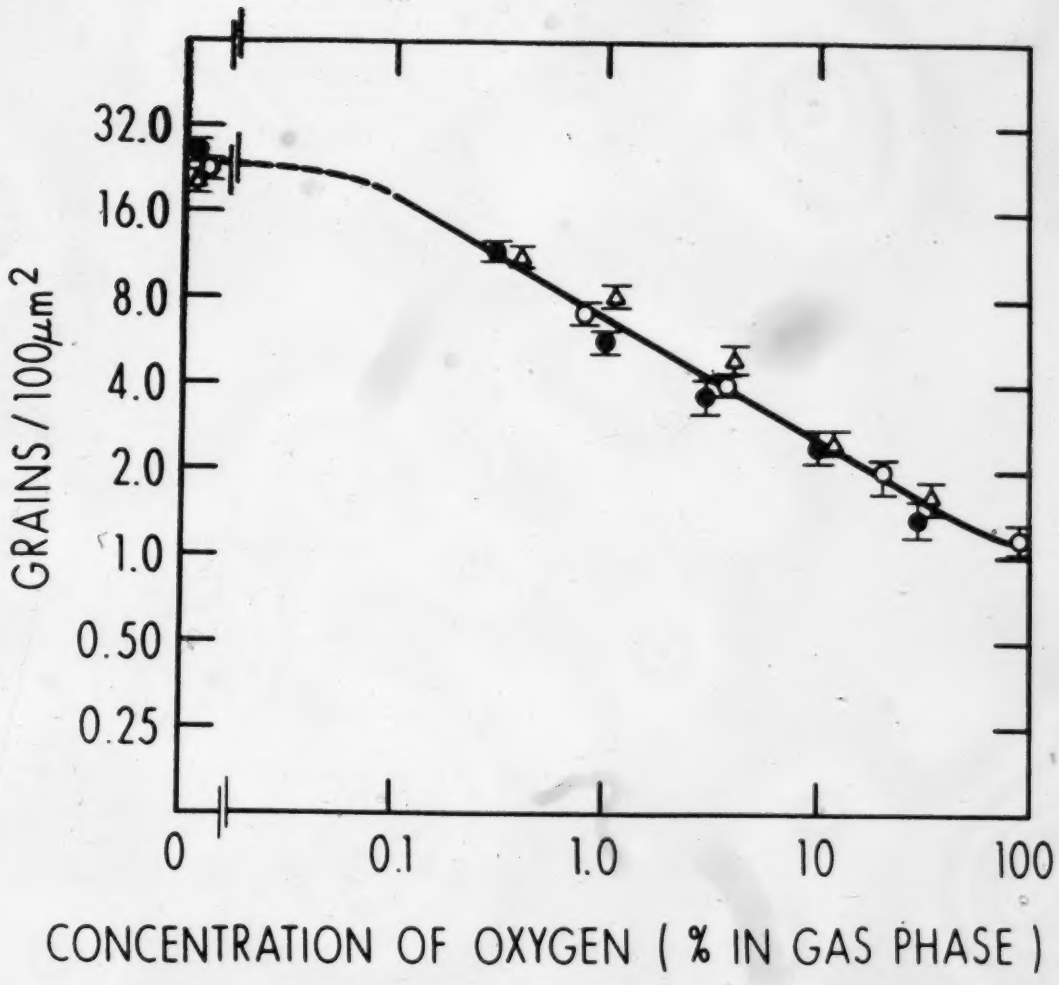

FIGURE 8: The rate of ^{14}C-Misonidazole binding to mouse liver vs. tissue pO_2. The pooled data from three individual experiments are shown. The standard error is indicated for each point.

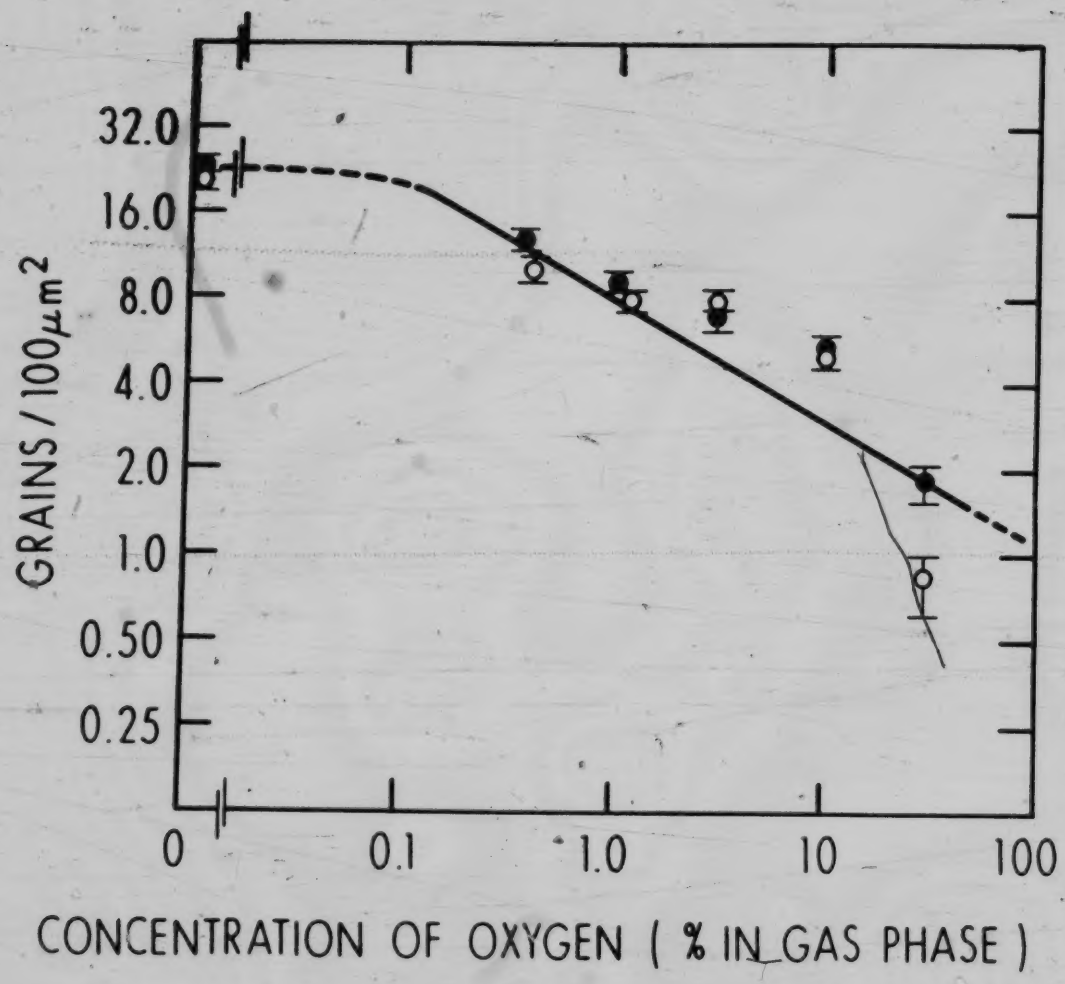

FIGURE 9: The rate of ^{14}C-Misonidazole binding to mouse brain vs. tissue pO_2. The pooled data from two individual experiments are shown. The standard error is indicated for each point.

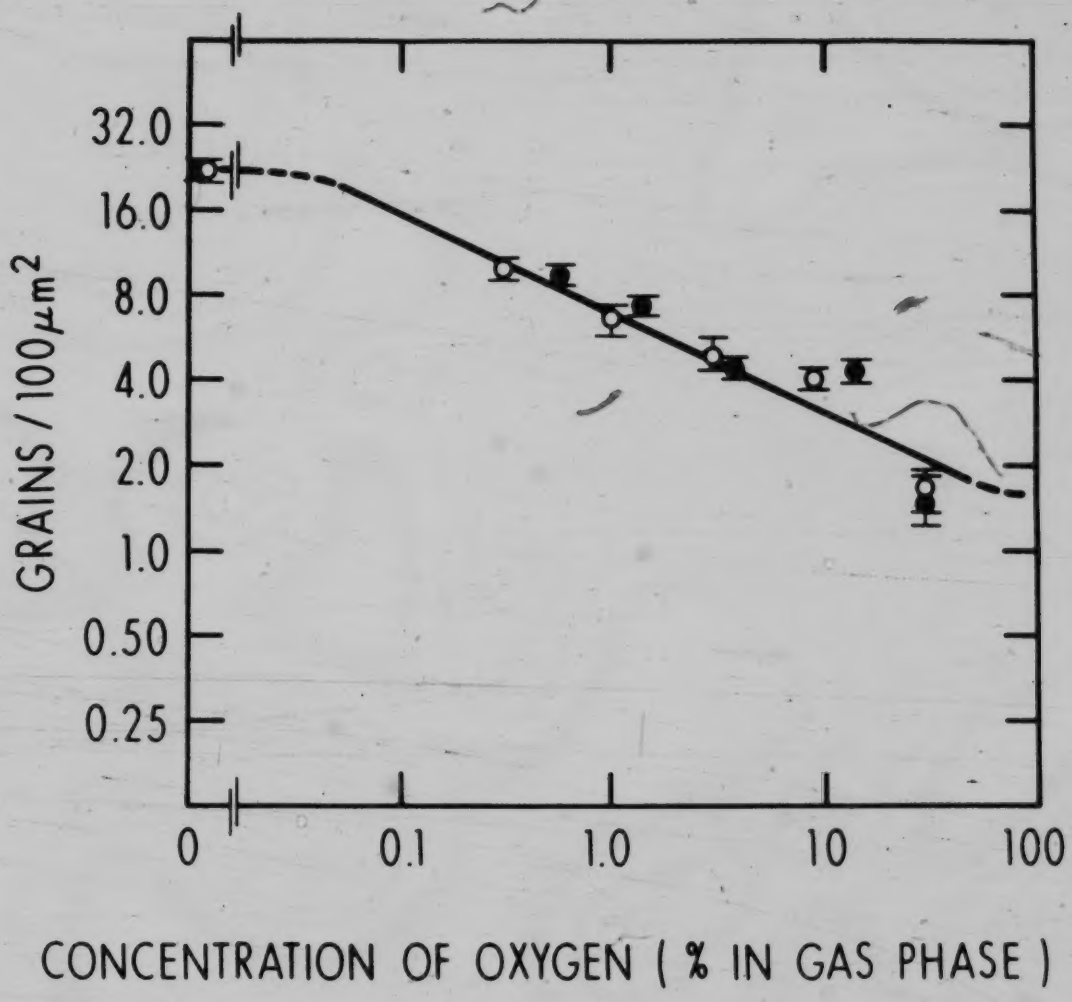

FIGURE 10: The rate of ^{14}C-Misonidazole binding to mouse heart vs. tissue pO_2. The pooled data from two individual experiments are shown. The standard error is indicated for each point.

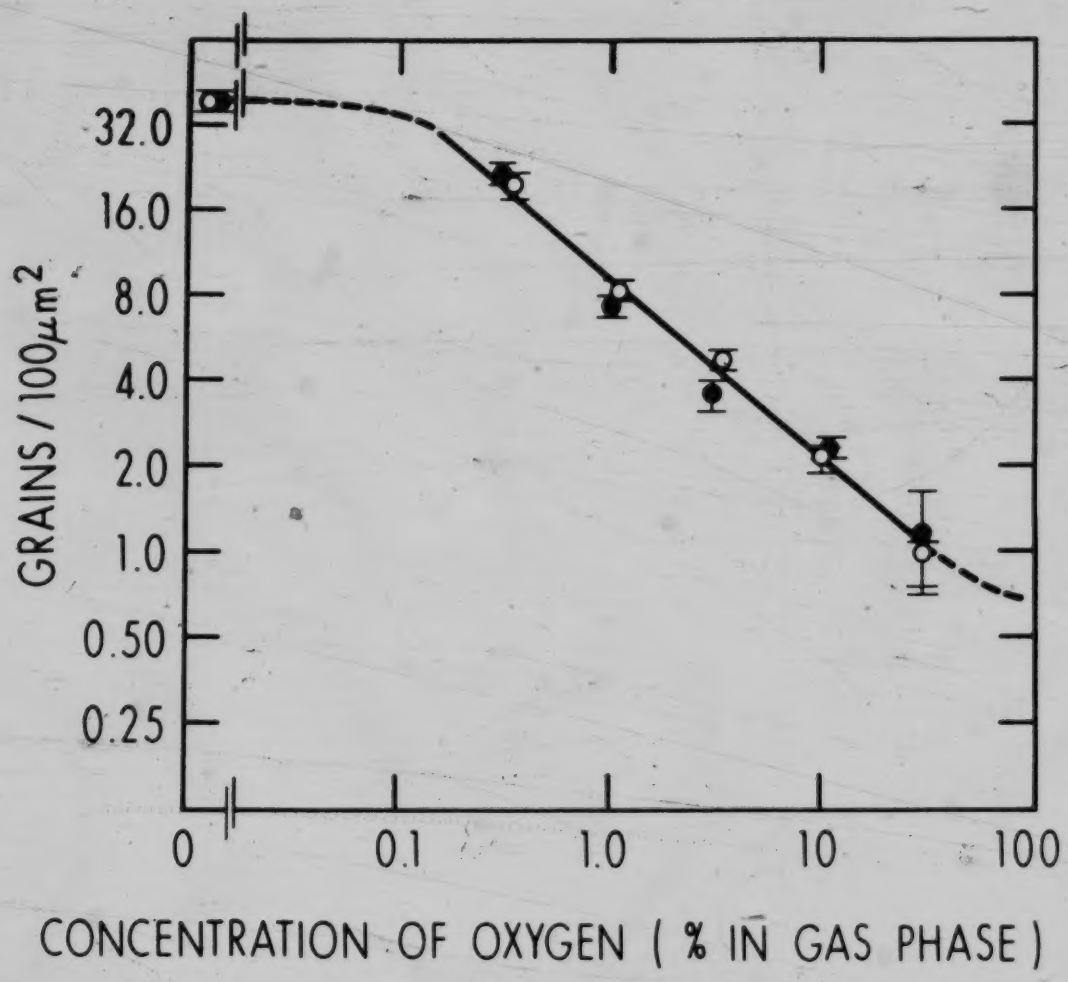

FIGURE 11: The rate of ^{14}C-Misonidazole binding to EMT-6 tumor vs. tissue pO_2. The pooled data from two individual experiments are shown. The standard error is indicated for each point.

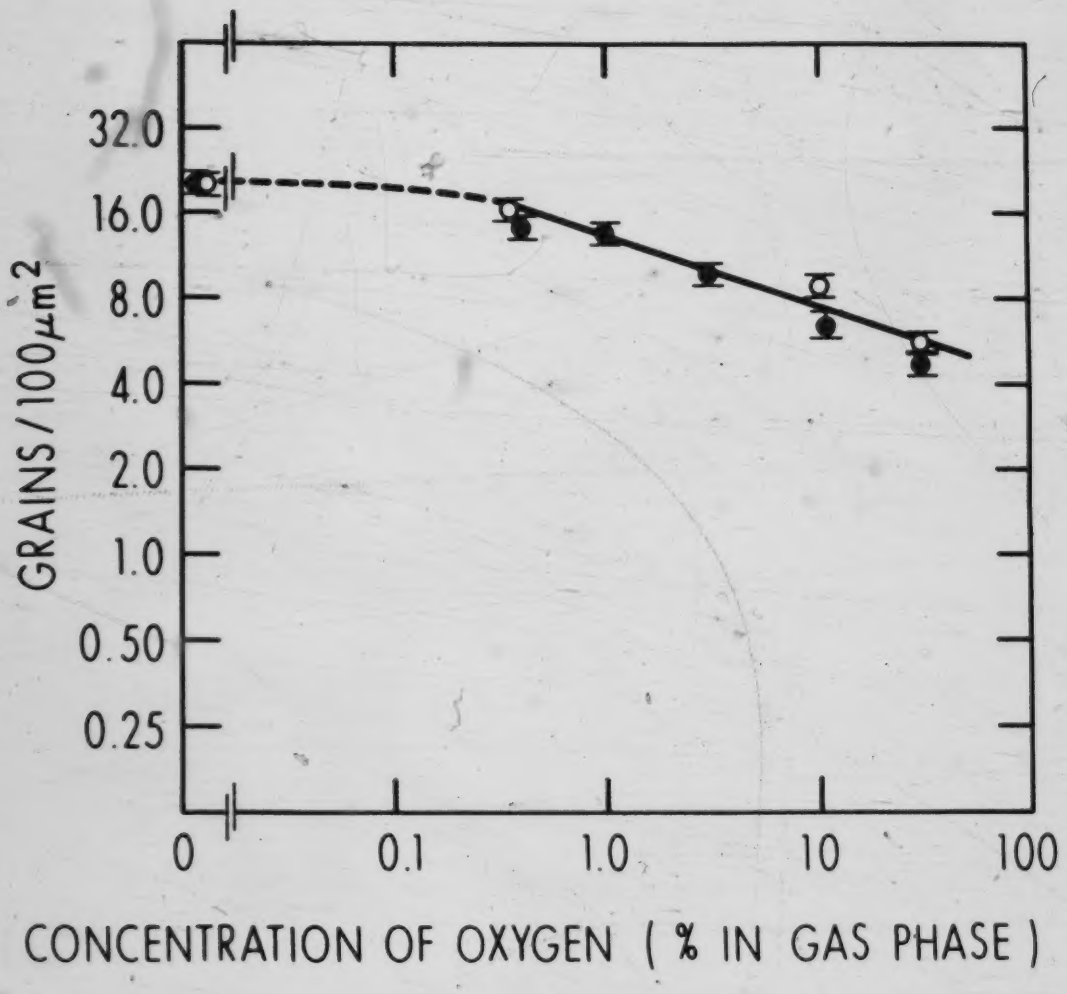

FIGURE 12: The rate of ^{14}C-Misonidazole binding to mouse kidney vs. tissue pO_2. The pooled data from two individual experiments are shown. The standard error is indicated for each point.

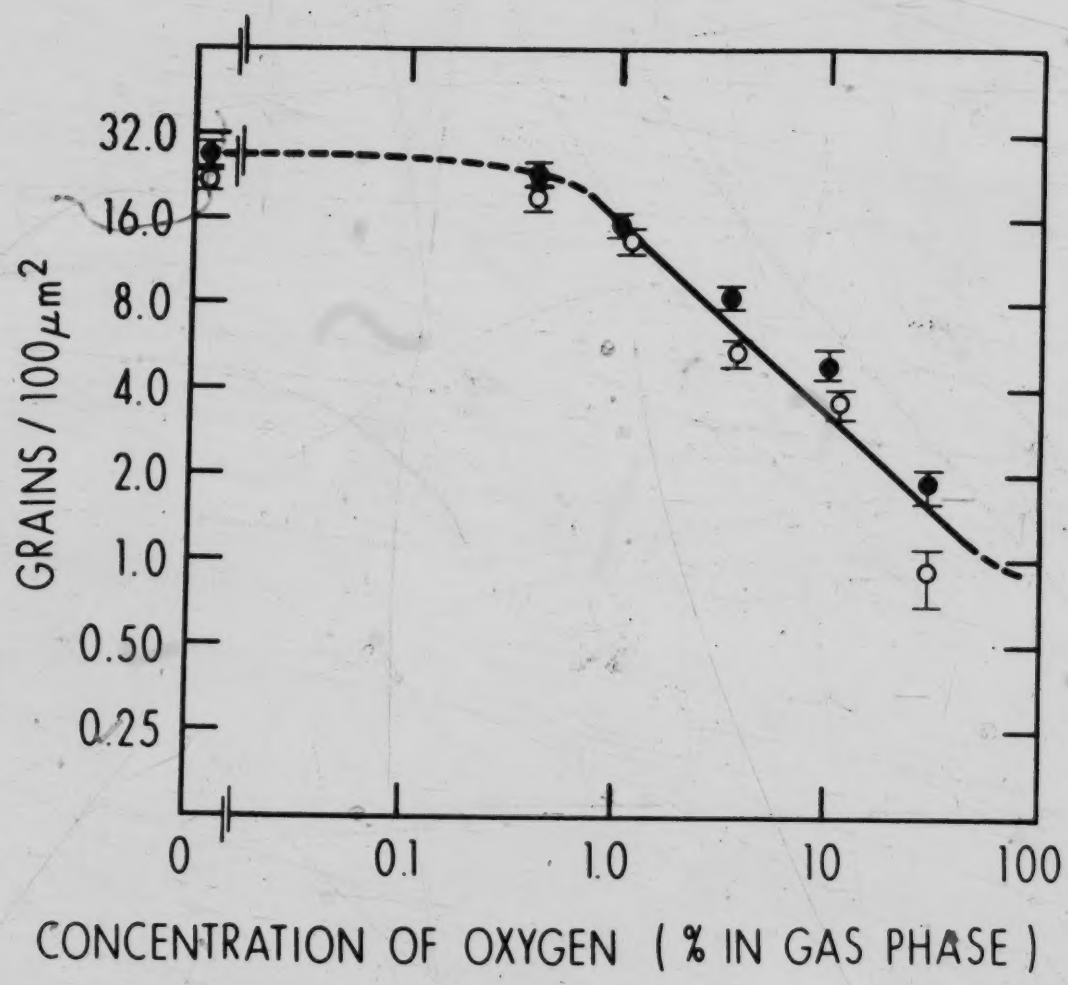

FIGURE 13: The rate of ^{14}C-Misonidazole binding to mouse spleen vs. tissue pO_2. The pooled data from two individual experiments are shown. The standard error is indicated for each point.

TABLE 2

K_m VALUES FOR MOUSE TISSUES ESTIMATED FROM STANDARD BINDING CURVE

	HYPOXIC BINDING RATE* GRAINS/100 μm^2	30% O_2 BINDING RATE GRAINS/100 μm^2	K_m
BRAIN	22.5	1.5	0.4%
KIDNEY	21.5	6.0	1.0%
LIVER	24.0	1.5	0.3%
TUMOR	40.0	1.0	0.3%
SPLEEN	27.5	1.5	1.3%
HEART	24.0	1.5	0.25%

* assuming hypoxic binding as maximum and 30% binding as minimum

K_m = half-maximum

although the maximum and minimum binding rates were similar to other normal tissues.

The binding pattern of grains in N_2 and 30% oxygen is shown for individual tissues in Plates 4 to 15. Although attempts were made to apply the emulsion as a single layer this was not always the case, therefore it was necessary to count grains in all layers of the emulsions when making an accurate determination. In 30% oxygen fewer grains bind at the surface of each tissue and the number of grains increases towards the center of the cube. An example of the increase in grain density with depth from the tissue surface is shown in Figure 14. This increase correlates with intracellular oxygen concentration which is determined by oxygen diffusion into and consumption by the cube.

In N_2 there is uniform binding of grains throughout the cube right to the cube surface. This indicates that the outer cells have not been damaged by mechanical procedures during handling. This is an important observation since it is the outer layer of cells that is being used in the autoradiographic analysis of absolute binding rates.

Due to the inherent biological variability that is associated with using autoradiographic techniques it is important that when repeating experiments every attempt is made to accurately duplicate all conditions of the experiment to eliminate possible sources of error. In this regard it is important that 1) the thickness of the emulsion on the slide remains consistent; 2) the exposure time is kept constant; 3) the same person does all grain counting to eliminate differences in the interpretation of grain numbers in heavily labelled areas; 4) an independent check using liquid scintillation counting is made of the

PLATE 4

Grain density at surface of mouse liver cube incubated in nitrogen. Cube surface is denoted by arrow. Magnification 1056X.

PLATE 5

Grain density at surface of mouse liver cube incubated in 30% oxygen. Cube surface is denoted by arrow. Magnification 1056X.

PLATE 6

Grain density at surface of mouse brain cube incubated in nitrogen. Cube surface is denoted by arrow. Magnification 1056X.

PLATE 7

Grain density at surface of mouse brain cube incubated in 30% oxygen. Cube surface is denoted by arrow. Magnification 422X.

PLATE 8

Grain density at surface of mouse heart cube incubated in nitrogen. Cube surface is denoted by arrow. Magnification 1056X.

Note: Although it appears that binding decreases at the surface of the cube, it is in fact uniform. It is difficult to show the grains present in all layers of the emulsion in a single photograph. The grains in all layers are taken into account during counting.

PLATE 9

Grain density at surface of mouse heart cube incubated in 30% oxygen. Cube surface is denoted by arrow. Magnification 422X.

PLATE 10

Grain density at surface of EMT-6 tumor cube incubated in nitrogen. Cube surface is denoted by arrow. Magnification 1056X.

PLATE 11

Grain density at surface of EMT-6 tumor cube incubated in 30% oxygen. Cube surface is denoted by arrow. Magnification 1056X.

PLATE 12

Grain density at surface of mouse kidney cube incubated in nitrogen. Cube surface is denoted by arrow. Magnification 1056X.

PLATE 13

Grain density at surface of mouse kidney cube incubated in 30% oxygen. Cube surface is denoted by arrow. Magnification 1056X.

PLATE 14

Grain density at surface of mouse spleen cube incubated in nitrogen. Cube surface is denoted by arrow. Magnification 1056X.

PLATE 15

Grain density at surface of mouse spleen cube incubated in 30% oxygen. Cube surface is denoted by arrow. Magnification 1056X.

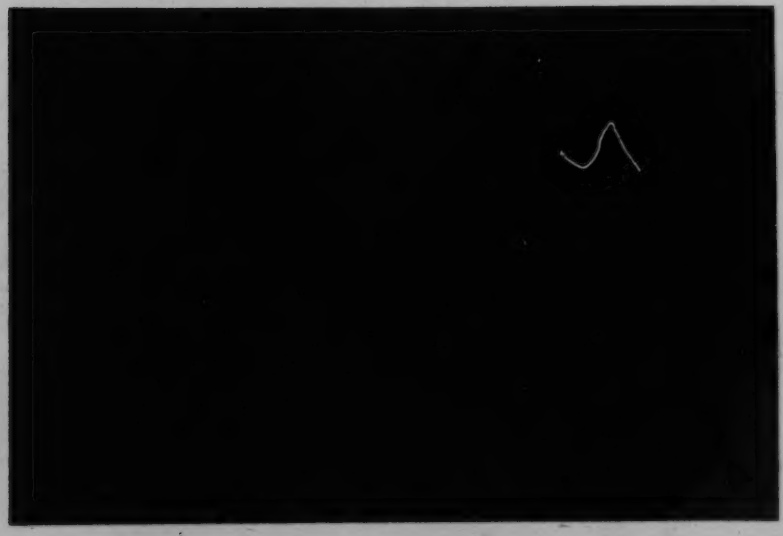

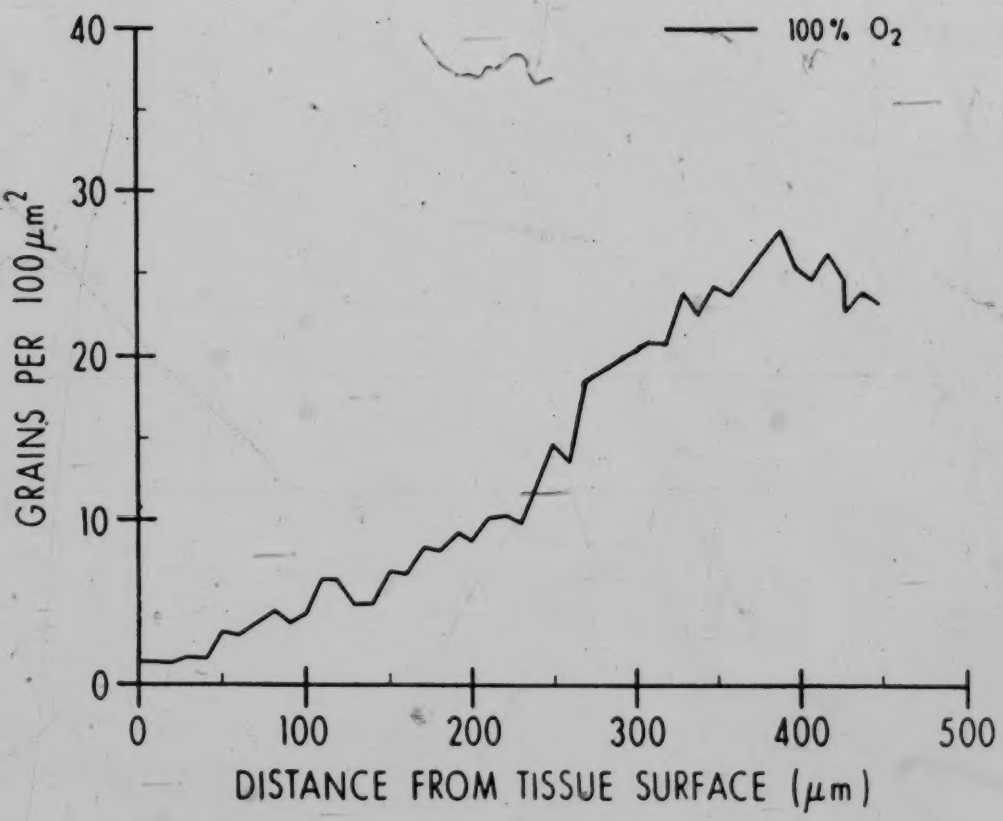

FIGURE 14: Grain density over liver tissue vs. distance from tissue surface.

amount of drug in the petri dishes; 5) the size of the tissue cubes used remains consistent; 6) the exact gas level in the chambers is accurately measured both before and after the incubation period; 7) background grains found in the emulsion are quantified and subtracted from all values; 8) a large number of counts are done so that an accurate average determination can be made and 9) the section thickness is consistently maintained at 4 μm.

A potential source of error that must be considered when using the cube technique is the possibility that a certain amount of discrepancy exists between the pO_2 measured with microelectrodes in the incubating medium and the actual pO_2 that exists in the outer cell layer of the cube. While the assumption made in the binding experiments is that these two values are the same it should be pointed out that in actual fact the medium pO_2 is only a maximum value for the outer cell layer. Studies have shown that depletion of oxygen due to oxygen consumption across the small unstirred layer of medium next to the cube surface could mean that the pO_2 of the outer cell layer is lower than the pO_2 of the surrounding medium (57). This effect appears to be most prominent at low levels of oxygen where it is calculated that the maximum discrepancy is a factor of 3 (57). In terms of the standard curves which were determined for the different tissues, this could result in a shift of the curves to the left and a subsequent change in the K_m value for the tissue.

CHAPTER 5

RESULTS AND DISCUSSION

The Binding of ^{14}C-Misonidazole to Mouse Tissues *in vivo*

Experiments were designed to determine if the binding of ^{14}C-MISO to mouse tissues *in vivo* could be altered by subjecting the animals to hypoxic or hyperoxygenated conditions during the 3 hour labelling period. After labelling *in vivo* the excised tissues were cut in half with one half being used for autoradiographic analysis and the other for liquid scintillation counting. The autoradiographic results are shown in Table 3. No significant change in grain density was observed in brain, liver, muscle or EMT-6 tumor when the breathing condition of the animal was switched from room air to either hypoxic (8% O_2 + 92% N_2) or hyperoxygenated (95% O_2 + 5% CO_2) conditions.

The results obtained with the liquid scintillation counting technique are shown in Table 4. A slight increase from .8 to 2.0 dpm/100 mg was observed for brain tissue in hypoxic conditions. No significant changes were observed in the average dpm/100 mg for mouse liver, muscle or EMT-6 tumor. It would appear from these results that the mice were able to compensate physiologically when subjected to acute environmental changes in oxygen tension, over a range of 8% - 95%, so that the actual pO_2 of the tissues did not change. This would explain why no significant differences in ^{14}C-MISO binding were observed. This compensation was most obvious in hypoxic conditions, where the animals conserve oxygen by becoming very inactive and increase their breathing rate to supply an adequate amount of oxygen to

TABLE 3

AVERAGE GRAIN DENSITY/1200 μm^2 AREA FOR MOUSE TISSUES LABELLED IN VIVO WITH 50 μM ^{14}C-MISO

TISSUE	BREATHING CONDITION		
	95% O_2 + 5% CO_2	AIR	8% O_2 + 92% N_2
Liver	107 ± 30	112 ± 53	121 ± 23
Brain	23 ± 11	21 ± 5	13 ± 5
Muscle	8 ± 2	20 ± 14	23 ± 16
Tumor			
Light Label	38 ± 15	42 ± 18	16 ± 7
Dense Label	569 ± 46	329 ± 98	399 ± 95

TABLE 4

AVERAGE dpm/100 mg ($\times 10^4$) FOR MOUSE TISSUES LABELLED IN VIVO WITH 50 μM ^{14}C-MISO

	BREATHING CONDITION		
TISSUE	95% O_2 + 5% CO_2	AIR	8% O_2 + 92% N_2
Liver	5.8	6.1	4.2
Brain	0.8	0.8	2.0
Muscle	0.7	0.6	0.7
Tumor	10.0	6.7	10.3

the tissues. Several other physiological mechanisms exist that enhance an animal's ability to cope with short-term exposure to hypoxic conditions. An increase 2,3-diphosphoglycerate (2,3-DPG) stabilizes the deoxygenated form of hemoglobin, resulting in decreased oxygen affinity of hemoglobin and therefore enhanced oxygen release to the tissues (4). Enhanced oxygen supply to the tissues can also be achieved by altering the blood flow to result in an increased cardiac output (58).

In a second experiment, the in vivo aerobic binding of ^{14}C-MISO to brain, liver and EMT-6 tumor was used to estimate the in vivo pO_2 of these tissues using the standard curves obtained in Chapter 4. Autoradiographic analysis was used to determine the average grain density/1200 μm^2 area for brain, liver and densely labelled or lightly labelled tumor in vivo (see Table 5). We have assumed that the densely labelled tumor in vivo is indicative of chronic hypoxia. Densely labelled tumor was assigned a value of 1.0 and the other values were expressed as ratios with respect to hypoxic tumor. The ratios for two independent experiments were averaged. To determine the average grains/100 μm^2 area, a ratio of 1.0 was equated to 40 grains/100 μm^2, the maximum binding observed to tumor cubes in vitro labelled in N_2 (Figure 11). The ratios obtained for brain, liver and lightly labelled tumor were normalized by multiplying each value by a factor of 40 to obtain the average grains/100 μm^2 area. These values were then fitted on the appropriate standard curve (Chapter 4) and the approximate in vivo pO_2 for each tissue was determined. As outlined in Table 5 the in vivo pO_2 values determined using this method were: liver - .7% (5.3 mm Hg), brain - 20% (152 mm Hg), lightly labelled (aerobic) tumor - 10%

TABLE 5

ESTIMATED pO_2 LEVELS FOR MOUSE BRAIN, LIVER AND EMT-6 TUMOR

	EXPT 1 GRAINS/ 1200 μm^2	RATIOS	EXPT 2 GRAINS/ 1200 μm^2	RATIOS	MEAN (EXPT 1 & 2)	GRAINS/ 100 μm^2	ESTIMATED pO_2
BRAIN	21 + 2.2	.06	10 + 1.1	.05	.05	2.4	20% (152 mm Hg)
LIVER	112 + 23.7	.34	29.8 + 3.0	.16	.25	10.0	.7% (5.3 mm Hg)
TUMOR DENSE LABEL	329 + 43.9	1.0	181.6 + 16.5	1.0	1.0	40	<.1% (.76 mm Hg)
TUMOR LIGHT LABEL	26.4 + 5.3	.08	6.6 + 1.2	.03	.05	2.3	10% (76 mm Hg)

(76 mm Hg) and densely labelled tumor - .1% (.76 mm Hg). For densely labelled tumor it was necessary to estimate an approximate pO_2 range since from the standard curve (Figure 10) a maximum binding of 40 grains/100 μm^2 area is possible over a concentration of oxygen ranging from 0.01 - 0.1% (.076 - .76 mm Hg). It would appear that the amount of sensitizer adduct bound/100 μm^2 area may be a relatively sensitive technique for the measurement of in vivo tissue pO_2 levels if standard curves can be generated in vitro utilizing short-term tissue culture.

Several factors must be discussed which could affect the precision of the measurements made using the sensitizer adduct technique. One problem, which could affect the comparison between in vivo and in vitro binding to tissues, is that there is no way to accurately determine what the precise in vivo drug concentration was during the multiple labelling experiments. Although we can make a reasonable estimate from the weight of the mouse and the amount of drug injected to maintain the drug concentration in the plasma at 10 µg/gm (50 µm) for 3 hours, it could be argued that the in vitro and in vivo drug concentrations are not necessarily identical. We do know, however, from biodistribution studies by Garrecht and Chapman (21) that the distribution of ^{14}C-MISO in the plasma and other normal tissues for the 3 hour period is approximately the same and that at least there would be no large difference in the amount of drug to which each tissue was exposed in vivo. That this level was equivalent to 50 µm was not determined.

In Chapter 4, the problems associated with the assumption that the pO_2 in the medium was the same as the pO_2 in the outer cell layer of the tissue cube were discussed. It was suggested that the maximum error

involved, most prominent at low oxygen tensions, was that the pO_2 of the outer cell layer might be up to a factor of 3 lower than the pO_2 of the surrounding medium. If this is the case, then the standard curves would shift to the left at low pO_2 levels with little change being observed in the curve at higher oxygen tensions. This would result in an error for the K_m value of about 50%. Since the in vivo pO_2 values were estimated using the part of the curve that is least affected by error it is likely that the maximum error expected with the sensitizer adduct technique would be less than 50%. For example, the pO_2 of brain tissue could exist in a range of 10 - 20% (76 - 152 mm Hg).

CHAPTER 6

GENERAL DISCUSSION AND CONCLUSIONS

In an attempt to determine why mouse liver *in vivo* binds ^{14}C-MISO at a much higher rate than other normal tissues, the studies presented in this thesis have characterized the binding of ^{14}C-MISO to both liver cells and liver tissue cubes *in vitro*. From the results presented in Chapter 3 it is evident that the characteristics of metabolic binding of ^{14}C-MISO to isolated liver cells is qualitatively similar to EMT-6 tumor cells, mouse hepatoma cells and V79 fibroblast cells. When hepatocytes are incubated in aerobic conditions little or no binding of drug is observed. It is thought that the presence of oxygen blocks the metabolic reduction of the MISO nitro group which is a necessary step in the binding process (59). When liver cells were incubated with MISO under extremely hypoxic conditions the binding rates were increased significantly (average binding rate at 50 μM = 25.1 pmoles/10^6 cells/hr). A logarithmic plot of liver cell binding rate vs. ^{14}C-MISO concentration showed that the kinetics of binding in N_2 was consistent with half-order kinetics as described by Chapman et al. (50) and Koch et al. (60) for EMT-6 cells and V79 cells. Half-order kinetics were also observed in the binding to mouse hepatoma cells.

When comparing the absolute rate of binding determined for mouse liver cells to EMT-6 cells, V79 cells or mouse hepatoma cells it was observed that under hypoxic conditions liver cells exhibited the lowest binding rate at all drug concentrations studied. These results suggest that liver cells do not possess a unique complement of nitroreductase

enzymes, compared to normal fibroblast cells or tumor cells, that would account for their elevated binding rate observed *in vivo*.

Evidence to support this conclusion was obtained in experiments which examined the binding of ^{14}C-MISO to mouse liver, spleen, heart, kidney, brain and EMT-6 tumor tissue cubes under controlled oxygen conditions *in vitro*. The results of these studies, which were presented in Chapter 4, showed that the K_m value for half-maximal binding and the absolute rates (grains/100 μm^2) observed for liver were not significantly different from those of other tissues such as brain, heart and tumor. These results are consistent with the data obtained with isolated liver cells that suggest that liver does not possess a unique complement of nitroreductase enzymes when compared to other normal tissues. Based on these findings it would be expected that liver *in vivo* should exhibit similar MISO binding characteristics as heart or brain, provided that the *in vivo* pO_2 of these tissues was the same.

As described earlier, however, the biodistribution studies of ^{14}C-MISO binding in Balb/C mice by Garrecht and Chapman (21) found that *in vivo* there was a 4 - 15 fold elevation in the binding of ^{14}C-MISO to liver when compared to all other normal tissues. It would appear from the results of binding studies at both the tissue and cellular level *in vitro* that the elevated binding observed to liver *in vivo* is due to some other factor such as the organ existing at a pO_2 which is significantly lower than other normal tissues.

The results obtained with both isolated hepatocytes and liver cubes seem to favour the interpretation that oxygen is the most important factor determining the rate of MISO binding to liver tissue.

It is important, however, to point out an alternative explanation which should be considered. The liver is actively involved in the biosynthesis of lipids and as a result there is a high NADPH/NADP ratio in the cytoplasm of liver cells. It is possible, therefore, that the increased rate of MISO binding observed to liver *in vivo* could be due to the presence of a highly reduced cytoplasmic environment in individual cells which is somehow immediately altered upon tissue excision and hepatocyte purification.

The studies presented in Chapter 5 of this thesis examined the feasibility of using the binding of sensitizer adducts to mouse tissue cubes *in vitro* as a technique to estimate the pO_2 of tissues at the cellular level *in vivo*. An examination of the standard curves presented for six different tissues in Chapter 4 shows that the autoradiographic results of 2 - 3 independent experiments were reasonably reproduced at all oxygen concentrations for every tissue studied. When attempting to relate the *in vivo* grain counts to the standard pO_2 curves the results were normalized to a known point such as densely labelled and presumably chronically hypoxic tumor, as outlined in Chapter 5. In spite of the problems discussed in Chapter 5, it would appear from the pO_2 estimates obtained using this technique that it provides a reliable and sensitive method for estimating tissue pO_2 at the cellular level within a factor of 2. In concordance with the conclusions reached from the *in vitro* cell and tissue binding studies, our measurements determined an *in vivo* pO_2 for liver of 0.7% (5.32 mm Hg). When comparing this value to that obtained for brain, which was approximately 20% oxygen (152 mm Hg), it is clear that, *in vivo*, liver exists at a considerably reduced oxygen tension.

There is increasing evidence that some normal tissues may have considerably reduced *in vivo* pO_2 levels. Alkaline elution experiments by Meyn and Jenkins (61) have measured the efficiency of DNA strand break formation in normal and tumor tissues of mice in an attempt to determine the radiosensitivities of tissues *in vivo* and *in vitro*. When DNA strand break formation was measured for isolated cells irradiated *in vitro* it was found that all the cells, including those from bone marrow, spleen, brain, kidney, testes, liver and gut, had similar sensitivities within experimental error (61). When these same tissues were irradiated *in vivo* and the tissues then removed and analyzed by alkaline elution, Meyn found that the sensitivities of the normal tissues were not uniform but varied by as much as a factor of 2 - 4 (61). The most sensitive tissue with respect to single strand break formation was bone marrow while the most radioresistant tissues were gut and liver.

In comparison to the results obtained *in vitro*, the normal cells irradiated *in vivo* were more resistant to radiation by factors of 2 - 4. Since radioprotection is afforded by a lack of oxygen, Meyn concluded from these results that the increased resistance observed *in vivo* could be evidence for some normal tissues existing at relatively low oxygen tensions. Interestingly, out of all the tissues studied, liver and gut were the most radioresistant *in vivo* (61). These results support our conclusion that liver may exist at a lower pO_2 than other normal tissues.

Further *in vitro* evidence supporting the possibility that tissues exist at low oxygen tensions comes from studies which examined the

effect of reduced oxygen tensions on the plating efficiencies of both normal and neoplastic cell lines in long and short-term culture. A comparison of cell culture in standard oxygen conditions (20%) and reduced oxygen conditions (1 - 5%) demonstrated that plating efficiencies could be increased when the lower oxygen conditions were used. This phenomenon was observed by a number of investigators for a variety of cell lines including human melanoma cells (62,63), mouse embryo cells (64) and human fibroblasts (65). These results are interesting in that they imply that cells in normal tissues in vivo have adapted to an environment that has a pO_2 considerably lower that that of air.

Other investigators have also reported findings which suggest that some normal tissues are at low oxygen tensions. Hendry, in a recent review of the literature describes work showing an increase in the radiosensitivities of tissues in animals breathing oxygen at 1 atmosphere or greater pressure during irradiation instead of air (66). In his review, Hendry notes that these findings could be explained if the critical normal cells were at an oxygen tension of about 4 X lower than venous blood. Some critical normal tissues which have been shown to be moderately hypoxic radiobiologically using this method include the neuraxis in rats and laryngeal human cartilage (66). In addition to these studies, Bohlen has reported microelectrode measurements in the rat intestinal mucosa in which penetration of the cells at the base or apex of the villus with the electrode tip (2 μm in diameter) resulted in pO_2 values of less than 2 mm Hg (0.2% oxygen) (67).

Additional evidence to support the existence of low pO_2 levels in the liver comes from studies related to liver blood supply. Although

the liver is a well vascularized organ, it is supplied by a varying mixture of arterial and portovenous blood in the ratio 25%:75% (68). Measurement of the actual pO_2 of this blood supply shows that while the average pO_2 in the hepatic artery is 12.5% (95 mm Hg) this falls to only 3.9% (30 mm Hg) in the hepatic vein and 5.9% (45 mm Hg) in the portal vein (68). Clinical studies which have involved hepatic artery ligation have observed no hepatic necrosis as it appears that the liver can function adequately with only the venous blood as its sole supply (69,70).

A study by Lammertsma et al. used positron emission tomography to determine in vivo measurements of regional blood flow, oxygen utilization, oxygen extraction ratios and fractional blood volume in brain tumors and surrounding cerebral tissues (71). These studies showed that within the tumors there was no relationship between oxygen supply and utilization. In all cases the blood supply to cerebral tumors was in excess of their metabolic requirements for oxygen. It has not been determined if there are any normal tissues that are overperfused relative to their metabolic utilization of oxygen. If overperfusion does occur in liver it could provide an explanation as to why the pO_2 of the blood supplying the liver is considerably higher than the pO_2 value estimated for liver tissue by this sensitizer adduct technique.

CONCLUSIONS

The studies described in this thesis provide indirect evidence that liver cells in vivo do not possess a unique complement of nitroreductase enzymes that could account for its elevated binding of

^{14}C-MISO relative to other normal tissues. This suggests that liver *in vivo* exists at a pO_2 that is lower than some other normal tissues. Although admittedly laborious, it appears that the binding of sensitizer adducts to mouse tissue cubes *in vitro* can be developed as a sensitive and reliable measure of *in vivo* pO_2 levels and that standard binding curves can be generated for most normal tissues. The pO_2 of liver measured using this technique was 0.7% (5.32 mm Hg), which supports the conclusion that liver exists at a low pO_2 *in vivo*. The details of tissue pO_2 at the cellular level measured by this technique should prove useful in predicting the potential of magnetic resonance spectroscopy (MRS) and positron emission tomography (PET) procedures being developed for the measurement of tissue hypoxia (72). MRS and PET and other imaging procedures can currently measure signal averages from tissue volumes of 0.1 - 1.0 cm^3 (10^8 - 10^9 cells) (72).

BIBLIOGRAPHY

1. Gilbert, D.L. 1981. Oxygen and Living Processes - An Interdisciplinary Approach. Springer - Verlag, New York.

2. Neil, E. 1966. The development of ideas on oxygen transport by the blood. In: A Symposium on Oxygen Measurements in Blood and Tissues and Their Significance. Ed. J.P. Payne and D.W. Hill. J. & A. Churchill Ltd., London.

3. Molecular Oxygen in Biology - Topics in Molecular Oxygen Research. Ed. O. Hayaishi. North - Holland Publishing Company, Amsterdam, 1974.

4. Stryer, L. 1981. Biochemistry. W.H. Freeman and Company, San Francisco.

5. Weibel, E.R. 1984. The Pathway for Oxygen - Structure and Function in the Mammalian Respiratory System. Harvard University Press, Cambridge, Massachusetts and London, England.

6. Krog, J. 1974. Oxygen supply in aquatic forms. In: Molecular Oxygen in Biology. Topics in Molecular Oxygen Research. Ed. O. Hayaishi. North - Holland Publishing Company, Amsterdam.

7. Kennedy, K.A., Teicher, B.A., Rockwell, S. and Sartorelli, A.C. 1980. The hypoxic tumor cell: A target for selective cancer chemotherapy. Biochem. Pharmacol. 29: 1-8.

8. Chapman, J.D. 1979. Hypoxic sensitizers - Implications for radiation therapy. The New Eng. J. of Med. 26: 1429-1433.

9. Powers, W.E., Tolmach, L.J. 1963. A multicomponent X-ray survival curve for mouse lymphosarcoma cells irradiated in vivo. Nature 197: 710-711.

10. Elkind, M.M. 1970. Reoxygenation and its potential role in radiotherapy. In: Time and Dose Relationships in Radiation Biology as Applied to Radiotherapy. Springfield, VA. Clghse. Fed. Sci. Tech. Inf. 318-333.

11. Rockwell, S., Fischer, J.J., Martin, D.F. and Teicher, B.A. 1983. Artificial blood substitutes as adjuncts to cancer therapy. Cell Tissue Kinet. 16: 612.

12. Dische, S. 1979. Hyperbaric oxygen: the Medical Research Council trials and their clinical significance. Brit. J. Radiol. 51: 888-894.

13. Urtasun, R., Band, P., Chapman, J.D., Feldstein, M.L., Mielke, B. and Fryer, C. 1976. Radiation and high-dose metronidazole in supratentorial glioblastomas. New Eng. J. of Med. 294: 1364-1367.

14. Gerweck, L.E., Nygaard, T.G. and Burlett, M. 1979. Response of cells to hyperthermia under acute and chronic hypoxic conditions. Cancer Res. 39: 966-972.

15. Silver, I.A. 1966. The measurement of O_2 tension in tissues. In: A Symposium on Oxygen Measurements in Blood and Tissues and Their Significance. Ed. J.P. Payne and D.W. Hill. J. & A. Churchill Ltd., London.

16. Adams, G.E. 1973. Chemical radiosensitization of hypoxic cells. Br. Med. Bull. 29: 48-53.

17. Chapman, J.D., Reuvers, A.P., Borsa, J., Henderson, J.S. and Migliore, R.D. 1974. Nitroheterocyclic drugs as selective radiosensitizers of hypoxic mammalian cells. Cancer Chemother. Rep. 58: 559-570.

18. Dische, S., Saunders, M.I. and Lee, M.E. 1977. Clinical testing of the radiosensitizer Ro-07-0582: Experience with multiple doses. Br. J. Cancer 35: 567-569.

19. Chapman, J.D., Raleigh, J.A., Pedersen, J.E., Ngan, J., Shum, F.Y., Meeker, B.E. and Urtasun, R.C. 1979. Potentially three distinct roles for hypoxic cell sensitizers in the clinic. In: Radiation Research. Ed. S. Okada, M. Imamura, T. Terasima, H. Yamaguchi. Japanese Association for Radiation Research (JARR), Tokyo, Japan, 885-892.

20. Chapman, J.D., Franko, A.J. and Sharplin, J. 1981. A marker for hypoxic cells in tumors with potential clinical applicability. Br. J. Cancer 43: 546-550.

21. Garrecht, B.M. and Chapman, J.D. 1983. The labelling of EMT-6 tumors in Balb/C mice with ^{14}C-Misonidazole. Br. J. Radiol. 56: 745-753.

22. Peters, L.J., Miles, L. and Brock, W.A. 1983. Labelled pyruvate: A potential agent for imaging hypoxia in tumor. Radiat. Res. 94: 660-661.

23. Olive, P.L. and Durand, R.E. 1983. Fluorescent nitroheterocycles for identifying hypoxic cells. Cancer Res. 43: 3276-3280.

24. Ng, T.C., Evanochko, W.T. and Hiramoto, R.N. 1982. ^{31}P NMR spectroscopy of *in vivo* tumors. J. Mag. Resonance 49: 271-286.

25. Rappaport, C. and Howze, G.B. 1966. Dissociation of adult mouse liver by Sodium Tetraphenylboron, a potassium complexing agent. Proc. Soc. Exptl. Biol. Med. 121: 1010-1015.

26. Schapira, F., Delain, D. and Lacroix, Y. 1971. Multiple molecular forms of aldolase in fetal liver cell cultures: Action of dexamethasone. Enzyme 12: 545-552.

27. Umeda, M. and Saito, M. 1969. Carcinogenesis in tissue culture. XI. Cytotoxic effects of 4-dimethylaminoazobenzene and its derivatives on HeLa cells and on rat liver and kidney cells in culture. Jap. J. Exp. Med. 39: 601-613.

28. Howard, R.B. and Christensen, A.K. 1967. The enzymatic preparation of isolated intact parenchymal cells from [illegible] liver. J. Cell Biol. 35: 675-684.

29. Fry, J.R., Jones, C.A., Wiebkin, P., Bellemann, P. and Bridges, J.W. 1976. The enzymic isolation of adult rat hepatocytes in a functional and viable state. Anal. Biochem. 71: 341-350.

30. Berry, M.N. and Friend, D.S. 1969. High-yield preparation of isolated rat liver parenchymal cells. The Journal of Cell Biology 43: 506-520.

31. Strom, S.C., Jirtle, R.L., Jones, R.S., Novicki, D.L., Rosenberg, M.R., Novotny, A., Irons, G., McLain, J.R. and Michalopoulos, G. 1982. Isolation, culture and transplantation of human hepatocytes. J. Nat. Cancer Inst. 68: 771-775.

32. Berry, M.N., Farrington, C., Gay, S., Grivell, A.R. and Wallace, P.G. 1983. Preparation of isolated hepatocytes in good yield without enzymatic digestion. In: Isolation, Characterization and Use of Hepatocytes. Ed. Robert A. Harris and Neal W. Cornell. Elsevier Science Publishing Co., Inc.

33. Klaunig, J.E., Goldblatt, P.J., Hinton, D.E., Lipsky, M.M., Chacka, J. and Trump, B.F. 1981. Mouse liver cell culture. I. Hepatocyte isolation. In Vitro 17: 913-925.

34. Queral, A.E., DeAngelo, A.B. and Garrett, C.T. 1984. Effect of different collagenases on the isolation of viable hepatocytes from rat liver. Anal. Biochem. 138: 235-237.

35. Alley, M.C., Powis, G., Appel, P.L., Kooistra, K.L. and Lieber, M.M. 1984. Activation and inactivation of cancer chemotherapeutic agents by rat hepatocytes cocultured with human tumor cell lines. Cancer Res. 44: 549-556.

36. Stewart, D.J. and Inabu, T. 1979. N-Demethylation of aminopyrine in vivo and in the isolated hepatocyte of the rat. Biochem. Pharmacol. 28: 461-464.

37. Howard, R.B., Lee, J.C. and Pesch, L.A. 1973. The fine structure, potassium content, and respiratory activity of isolated rat liver parenchymal cells prepared by improved enzymatic techniques. J. Cell Physiol. 57: 612-658.

38. Asada-Kubota, M., Watanabe, J., Kanamura, S., Kanai, K. and Yoshikawa, M. 1982. Binding and internalization of ^{125}I-glucagon in hepatocytes of intact mouse liver. Exp. Path. 23: 95-101.

39. Le, P.T. and Mortensen, R.F. 1984. Mouse hepatocyte synthesis and induction of the acute phase reactant: serum amyloid P-component. In Vitro 20: 505-511.

40. Okigaki, T. 1977. A reproducible technique for rat liver culture. Tissue Culture Association Manual 3: 565-566.

41. Heine, V.I., Wilson, M.J. and Munoz, E.F. 1984. Characterization of rat liver cells transformed in culture by Dh-ethione. In Vitro 20: 291-301.

42. Sanders, S.W., Dukes, G.E., Gray, P. and Tolman, K.G. 1984. Toxicity of heparin in isolated rat hepatocytes. Biochem. Pharmacol. 33: 2223-2226.

43. Evarts, R.P., Marsden, E. and Thorgeirsson, S. 1984. Regulation of heme metabolism and cytochrome P-450 levels in primary culture of rat hepatocytes in a defined medium. Biochem. Pharmacol. 33: 565-569.

44. Reid, L.M. and Jefferson, D.M. 1984. Culturing hepatocytes and other differentiated cells. Hepatology 4: 548-559.

45. Lopez, M.P., Gomez-Lechon, M.J. and Castell, J.V. 1984. Glycogen synthesis in serum-free cultured hepatocytes in response to insulin and dexamethasone. In Vitro 20: 923-931.

46. Grisham, J.W. 1983. Cell types in rat liver cultures: Their identification and isolation. Molecular and Cellular Biochemistry 53/54: 23-33.

47. Klaunig, J.E., Goldblatt, P.J., Hinton, D.E., Lipsky, M., Knipe, S. and Trump, B. 1982. Morphologic and functional studies of mouse hepatocytes in primary culture. The Anatomical Record 204: 231-243.

48. Jirtle, R.L., Michalopoulos, G., McLain, J.R. and Crowley, J. 1981. Transplantation system for determining the clonogenic survival of parenchymal hepatocytes exposed to ionizing radiation. Cancer Res. 41: 3512-3518.

49. Deschenes, J., Valet, J.P. and Marceau, N. 1980. Hepatocytes from newborn and weanling rats in monolayer culture: Isolation by perfusion, fibronectin-mediated adhesion, spreading and functional activities. In Vitro 16: 722-730.

50. Chapman, J.D., Baer, K. and Lee, J. 1983. Characteristics of the metabolism-induced binding of misonidazole to hypoxic mammalian cells. Cancer Res. 43: 1523-1528.

51. Miller, G.G., Ngan-Lee, J. and Chapman, J.D. 1982. Intracellular localization of radioactively labelled misonidazole in EMT-6 tumor cells in vitro. Int. J. Radiat. Oncol. Biol. Phys. 8: 741-744.

52. Chapman, J.D., Blakely, E.A., Smith, K.C. and Urtasun, R.C. 1977. Radiobiological characterization of the inactivating events produced in mammalian cells by helium and heavy ions. Int. J. Radiat. Oncol. Biol. Phys. 3: 97-102.

53. Koch, C.J., Howell, R.L. and Biaglow, J.E. 1979. Ascorbate anion potentiates the cytotoxicity of nitro-aromatic compounds under hypoxic and anoxic conditions. Br. J. Cancer 39: 321-329.

54. Franko, A.J. 1985. Oxygen dependence of binding of misonidazole to rodent and human tumors in vitro. Not published.

55. Koch, C.J. 1975. Measurement of very low oxygen tensions in liquids: Does the extrapolation number for mammalian survival curves decrease after X-irradiation under hypoxic conditions? In: Cell Survival After Low Doses of Radiation: Theoretical and Clinical Applications. Ed. T. Alper. London: Institute of Physics, pp. 167-173.

56. Rogers, A.W. 1979. Techniques of Autoradiography. Elsevier North - Holland Biomedical Press, New York, NY.

57. Koch, C.J. 1985. Personal communication.

58. Prosser, C.L. 1973. Comparative Animal Physiology. Saunders College Publishing, Philadelphia. Third Edition.

59. Varghese, A.J., Gulyas, S. and Mohindra, J.K. 1976. Hypoxia dependent reduction of 1-(2-nitro-1-imidazolyl)-3-methoxy-2--propanol by Chinese hamster ovary cells and KHT tumor cells in vitro and in vivo. Cancer Res. 36: 3761-3765.

60. Koch, C.J., Stobbe, C.C. and Baer, K.A. 1984. Metabolism-induced binding of ^{14}C-misonidazole to hypoxic cells. Kinetic dependence on oxygen and misonidazole concentration. Int. J. Radiat. Oncol. Biol. Phys. 10: 1327-1331.

61. Meyn, R.E. and Jenkins, W.T. 1983. Variation in normal and tumor tissue sensitivity of mice to ionizing radiation-induced DNA strand breaks in vivo. Cancer Res. 43: 5668-5673.

62. Joyce, R.M. and Vincent, P.C. 1983. Advantage of reduced oxygen tension in growth of human melanomas in semi-solid cultures: Quantitative analysis. Br. J. Cancer 48: 385-393.

63. Gupta, V. and Krishan, A. 1982. Effect of oxygen concentration on the growth and drug sensitivity of human melanoma cells in soft-agar clonogenic assay. Cancer Res. 42: 1005-1007.

64. Richter, A., Sanford, K.K. and Evans, V.J. 1972. Influence of oxygen and culture media on plating efficiency of some mammalian tissue cells. J. Natl. Cancer Inst. 49: 1705-1711.

65. Taylor, W.G., Richter, A., Evans, V.J. and Sanford, K.K. 1974. Influence of oxygen and pH on plating efficiency and colony development of WI-38 and Vero cells. Exp. Cell Res. 86: 152-156.

66. Hendry, J.H. 1979. Quantitation of the radiotherapeutic importance of naturally hypoxic normal tissues from collated experiments with rodents using single doses. Int. J. Radiat. Oncol. Biol. Phys. 5: 971-976.

67. Bohlen, H.G. 1980. Intestinal tissue pO_2 and microvascular responses during glucose exposure. Am. J. Physiol. 238: 164-171.

68. Jungermann, K. and Katz, N. 1982. Functional hepatocellular heterogeneity. Hepatology 2: 385-395.

69. Athanasoulis, C.A., Pfister, R.C., Green, R.E. and Roberson, G.H. Interventional Radiology. W.B. Saunders Company, Philadelphia, London, Toronto.

70. Reuter, S.R. and Redman, H.C. 1977. Gastrointestinal Angiography. 2nd Edition. W.B. Saunders Company, Philadelphia, London, Toronto.

71. Lammertsma, A.A., Wise, R.J., Cox, T.C., Thomas, D.G. and Jones, T. 1985. Measurement of blood flow, oxygen utilization, oxygen extraction ratio, and fractional blood volume in human brain tumours and surrounding oedematous tissue. Brit. J. Radiol. 58: 725-734.

72. Urtasun, R.C., Koch, C.J., Franko, A.J., Raleigh, J.A. and Chapman, J.D. 1985. A novel technique for measuring human tissue pO_2 at the cellular level. Submitted to Br. J. Cancer.

73. Koch, C.J., Stobbe, C.C. and Bump, E.A. 1984. The Effect on the K_m for radiosensitization at $0^{\circ}C$ of thiol depletion by diethylmaleate pretreatment: Quantitative differences found using the radiation sensitizing agent misonidazole or oxygen. Rad. Res. 98: 141-153.

CURRICULUM VITA

NAME: DEBORA JOAN VAN OS-CORBY

PLACE OF BIRTH: Toronto, Ontario, Canada

YEAR OF BIRTH: 1960

POST SECONDARY EDUCATION AND DEGREES:

1979 - 1983	Trent University Peterborough, Ontario B.Sc. Honors
1984 - present	University of Alberta Edmonton, Alberta M.Sc. Candidate

HONORS AND AWARDS:

Trent University Scholarship
1979 - 1983

Biology Department Prize
1980

Midwives Prize
1980

Goodhead Scholarship
1981 - 1982

Summer Studentship
Ontario Cancer Institute
1982

President Symons Medal
1983

AHFMR Summer Studentship
1983

1967 Science and Engineering Scholarship
Natural Sciences and Engineering Council of Canada
1984 - 1986

Graduate Faculty Fellowship
University of Alberta
1985 - 1986

RELATED WORK EXPERIENCE:

Lab Demonstrator
Biology 110 (Zoology)
Trent University
1981 - 1982

Lab Demonstrator
Biology 382 (Physiology)
Trent University
1982 - 1983

Ontario Cancer Institute
Department of Medical Biophysics
Toronto, Ontario
Summer, 1982

Cross Cancer Institute
Department of Radiobiology
Edmonton, Alberta
Summer, 1983

ABSTRACTS AND PUBLICATIONS:

1. Corby, D.J. Binding of ^{14}C-Misonidazole to liver. Abstr. Western Canadian Radiobiology Workshop. Penticton, B.C., September 1984.

2. Van Os-Corby, D.J., Koch, C.J. and Chapman, J.D. Oxygen dependency of ^{14}C-Misonidazole binding to mouse liver in vivo and in vitro. Abstr. Id-9. Thirty-third Annual Meeting of the Radiation Research Society. May 5 - 9, 1985.

3. Van Os-Corby, D.J., Chapman, J.D. and Koch, C.J. Sensitizer adducts to mouse tissues as a probe for cellular pO_2. Abstr. Chemical Modifiers of Cancer Treatment. October 20 - 24, 1985.